iScience

CellPress
OPEN ACCESS

Article

β-chitosan attenuates hepatic macrophage-driven inflammation and reverses aging-related cognitive impairment

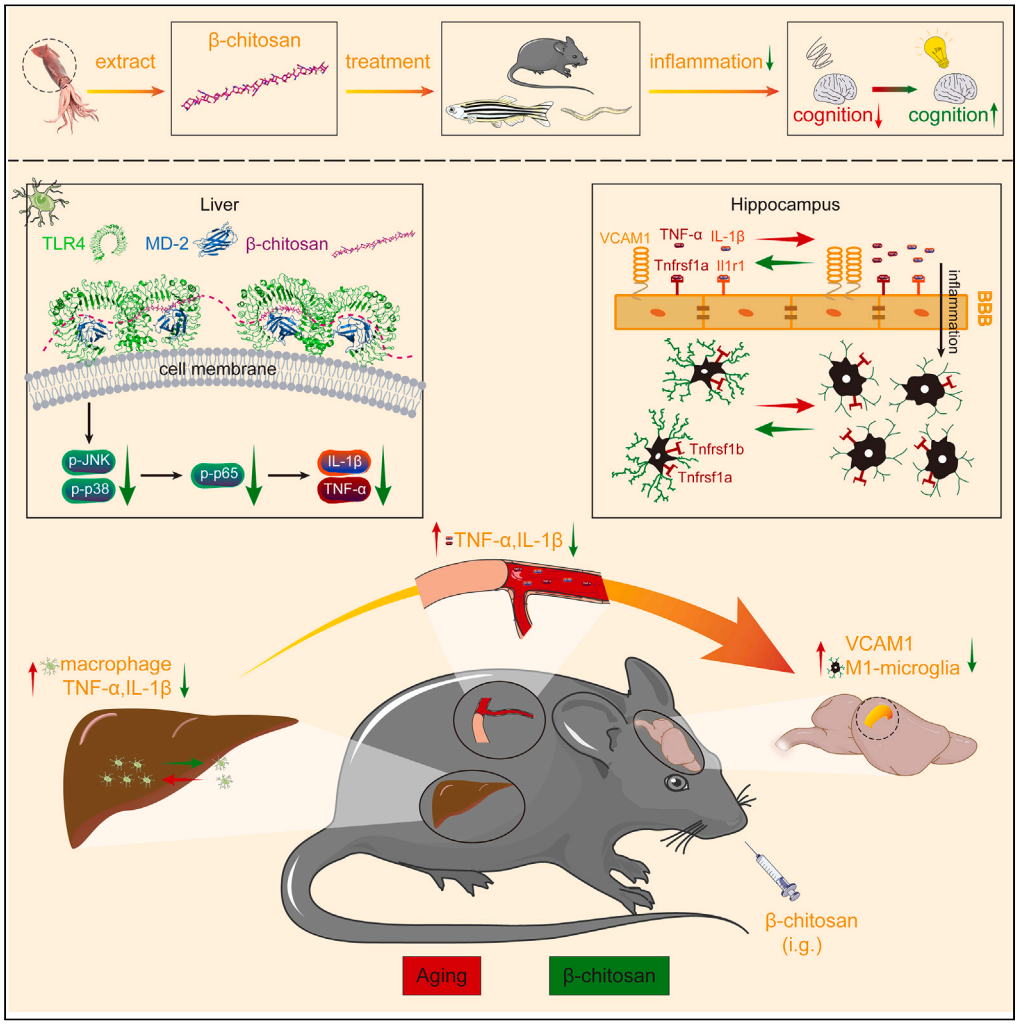

Chenming Zou, Ruihua Cai, Yunbing Li, ..., Gulimiran Alitongbieke, Yutian Pan, Sanguo Zhang

pyt1106@mnnu.edu.cn (Y.P.)
qiezihoutu@126.com (S.Z.)

Highlights

β-chitosan ameliorates age-related abnormal activation of macrophages through NF-κB pathway

β-chitosan reverses cognitive aging via improving chronic brain inflammation

β-chitosan helps decrease the occurrence of liver-brain inflammation caused by aging

β-chitosan improves the behavioral recovery of aged/LPS-stimulated zebrafish and *C. elegans*

Zou et al., iScience *27*, 110766
September 20, 2024
https://doi.org/10.1016/j.isci.2024.110766

iScience

CellPress
OPEN ACCESS

Article

β-chitosan attenuates hepatic macrophage-driven inflammation and reverses aging-related cognitive impairment

Chenming Zou,[1,2] Ruihua Cai,[1,2] Yunbing Li,[1,2] Yu Xue,[1,2] Guoguang Zhang,[3] Gulimiran Alitongbieke,[1,2] Yutian Pan,[1,2,*] and Sanguo Zhang[1,2,4,*]

SUMMARY

Recently, increasing evidence has shown the association between liver abnormal inflammation and cognition impairment, yet their age-related pathogenesis remains obscure. Here, our study provides a potential mechanistic link between liver macrophage excessive activation and neuroinflammation in aging progression. In aged and LPS-injected C57BL/6J mice, systemic administration of β-chitosan ameliorates hepatic macrophage-driven inflammation and reduces peripheral accumulations of TNF-α and IL-1β. Downregulation of circulatory pro-inflammatory cytokines then decreases vascular VCAM1 expression and neuroinflammation in the hippocampus, leading to cognitive improvement in aged/LPS-stimulated mice. Interestingly, β-chitosan treatment also exhibits the beneficial effects on the behavioral recovery of aged/LPS-stimulated zebrafish and *Caenorhabditis elegans*. In our cell culture and molecular docking experiments, we found that β-chitosan prefers shielding the MD-2 pocket, thus blocking the activation of TLR4-MD-2 complex to suppress NF-κB signaling pathway activation. Together, our findings highlight the extensive therapeutic potential of β-chitosan in reversing aged-related/LPS-induced cognitive impairment via the liver-brain axis.

INTRODUCTION

Along with economic development and continuous extension of life expectancy, the proportion of the elderly in the total population is expanding rapidly.[1] However, the increase in life expectancy does not mean healthy aging. There is a significantly increased cognitive deterioration as well as a greater susceptibility to the neurodegenerative diseases in the aging population.[2] The hippocampus has a vital role in learning and memory and has long been regarded as a crucial part of cognitive research.[3,4] Recently, plenty of studies have shown that microglia gradually become pro-inflammatory with aging and release inflammatory factors to damage neurons, resulting in neuroinflammation and cognitive impairment.[5]

The liver is the central organ of metabolism and plays a crucial role in toxin clearance, protein production, immune regulation, and decomposition of foreign compounds (including many drugs).[6,7] In order to perform these complex functions, the liver not only contains rare bone marrow–derived macrophages, but also the largest number of tissue-resident macrophages, termed Kupffer cells. They comprise about 25% of the non-parenchymal cells in the liver.[8,9] There are accumulative researches indicating hepatic macrophages display broad heterogeneity and sustain plasticity under different disease backgrounds, such as liver fibrosis,[10] liver cancer,[11] alcoholic hepatitis, and fatty liver.[12,13] Additionally, these liver disorders are associated with inflammation.

The geroscience considered that aging is constantly accompanied by chronic inflammation, which causes the onset of most age-related diseases.[14] Liver diseases in patients with nonalcoholic fatty liver,[15,16] hepatitis C,[17] liver fibrosis,[18] and chronic liver disease[19] affect brain health and cause cognitive deficits. Moreover, specific deletion of *IGF-I* gene in mouse liver also leads to cognitive impairment.[20] Recent studies showed that TNF-α and IL-1β in the peripheral blood circulatory system promoted the expression of vascular cell adhesion molecule 1 (VCAM1) in brain endothelial cells, which led to the activation of microglia and cognitive decline in mice.[21] Thus, we hypothesized that age-related low-grade chronic peripheral inflammation results in an increment of neuroinflammation in the hippocampus.

In this study, we used three kinds of biological models (mouse, zebrafish, and nematode with different ages) and LPS-challenged animals to explore the mechanistic linkage between peripheral inflammation and neuroinflammation. Chitosan has biodegradability, biocompatibility, and nontoxic properties, and is widely used in food, cosmetics, and biomedicine.[22] Two different structures of chitosan are classified

[1]The Engineering Technological Center of Mushroom Industry, Minnan Normal University, Zhangzhou 363000, China
[2]Fujian Fungal Active Substance Engineering Technology Center, Zhangzhou 363000, China
[3]School of Biological Science and Biotechnology, Minnan Normal University, Zhangzhou 363000, China
[4]Lead contact
*Correspondence: pyt1106@mnnu.edu.cn (Y.P.), qiezihoutu@126.com (S.Z.)
https://doi.org/10.1016/j.isci.2024.110766

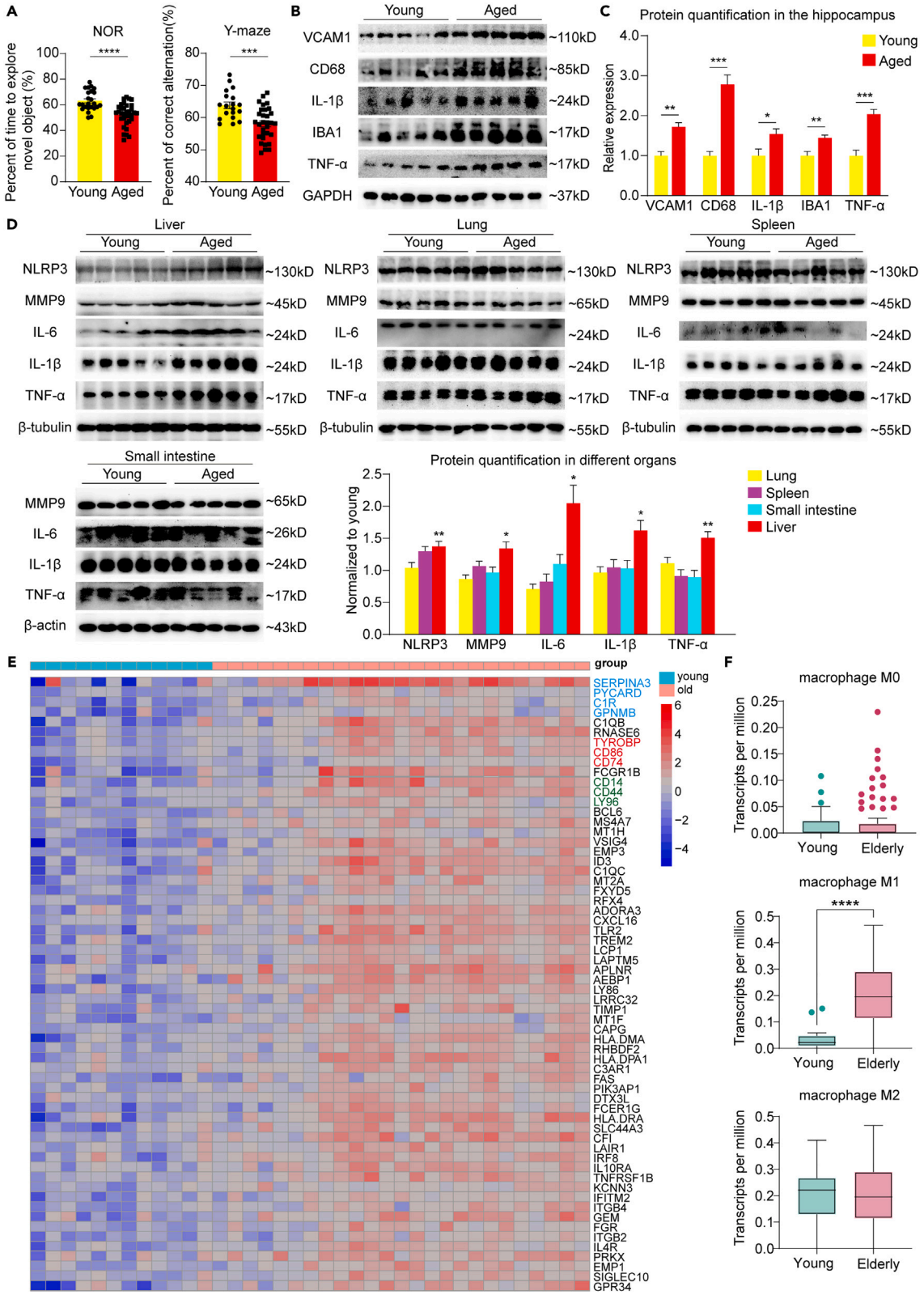
A
NOR
Percent of time to explore novel object (%)
Young Aged
Y-maze
Percent of correct alternation(%)
Young Aged
B
Young
Aged
VCAM1
CD68
IL-1β
IBA1
TNF-α
GAPDH
~110kD
~85kD
~24kD
~17kD
~17kD
~37kD
C
Protein quantification in the hippocampus
Young
Aged
Relative expression
VCAM1 CD68 IL-1β IBA1 TNF-α
D
Liver
Lung
Spleen
NLRP3
MMP9
IL-6
IL-1β
TNF-α
β-tubulin
~130kD
~45kD
~65kD
~24kD
~17kD
~55kD
Small intestine
MMP9
IL-6
IL-1β
TNF-α
β-actin
~65kD
~26kD
~24kD
~17kD
~43kD
Protein quantification in different organs
Normalized to young
Lung
Spleen
Small intestine
Liver
NLRP3 MMP9 IL-6 IL-1β TNF-α
E
group
young
old
SERPINA3
PYCARD
C1R
GPNMB
C1QB
RNASE6
TYROBP
CD86
CD74
FCGR1B
CD14
CD44
LY96
BCL6
MS4A7
MT1H
VSIG4
EMP3
ID3
C1QC
MT2A
FXYD5
RFX4
ADORA3
CXCL16
TLR2
TREM2
LCP1
LAPTM5
APLNR
AEBP1
LY86
LRRC32
TIMP1
MT1F
CAPG
HLA.DMA
RHBDF2
HLA.DPA1
C3AR1
FAS
PIK3AP1
DTX3L
FCER1G
HLA.DRA
SLC44A3
CFI
LAIR1
IRF8
IL10RA
TNFRSF1B
KCNN3
IFITM2
ITGB4
GEM
FGR
ITGB2
IL4R
PRKX
EMP1
SIGLEC10
GPR34
F
macrophage M0
Transcripts per million
Young Elderly
macrophage M1
Young Elderly
macrophage M2
Young Elderly

Figure 1. Hippocampus and liver exhibited aging-related inflammation

(A) Correct alternation performance in the Y-maze and percentage of time spent on exploring a new object in the novel object maze for young (3 months old; n = 19–24) and aged (12 months old; n = 31–34) mice.

(B) Detection of VCAM1, CD68, IL-1β, IBA1 and TNF-α expressions in hippocampi of young (4 months old) and aged (13 months old) mice by western blot. (C) Quantification analysis for the protein expressions in (B).

(D) The expressions of pro-inflammatory proteins NLRP3, MMP9, IL-6, IL-1β and TNF-α in the liver, lung, spleen and small intestine of young (4 months old) and aged (13 months old) mice were detected by western blot.

(E) Pearson ρ correlation matrix of transcriptome expression levels of young (n = 12, age <44 years) and elderly (n = 25, age 60 years or more) people hippocampi. Red: positive correlation; Blue: negative correlation. The blue-highlighted genes in the chart are associated with neurodegenerative diseases; the red-highlighted genes are associated with neuroinflammation; and the green-highlighted genes are associated with TLR4 signaling.

(F) The hepatic macrophage M0, M1 and M2 transcripts of young (n = 24, age 20–39 years) and elderly (n = 84, age 60–79 years) individuals. Data are presented as mean ± SEM, *p < 0.05, **p < 0.01, ***p < 0.001, ****p < 0.0001 by two-tailed t test.

into α- and β-type, in which α-chitosan is well known in various fields, but little is known about the β-chitosan, which has greater solubility, swelling, reactivity, and lesser crystalline nature than α-type.[23,24] Previously, we had found that β-chitosan could treat the lung inflammation caused by the S-RBD of COVID-19 virus in hACE2 mice.[25] Therefore, we took β-chitosan extracted from squid parietal bone as an anti-inflammatory agent to explore the potential intervention strategies for liver-brain inflammation treatment.

Herein, we evaluated the causal role of aging in promoting cognitive impairment and further identified that the liver macrophages contribute to the main source of peripheral inflammation, which may lead to impair hippocampal function and cognitive decline. β-chitosan exerts a strong beneficial effect on decreasing the occurrence of liver-brain inflammation caused by aging or exogenous stimulation, harnesses the abnormal activation of liver macrophages, and reduces the circulation of plasma inflammatory factors. It also reduces the expression of VCAM1 on the blood-brain barrier (BBB), and in turn ameliorates neuroinflammation and cognitive impairment.

RESULTS

Hippocampus and liver exhibited aging-related inflammation

To characterize age-related changes in cognition, we first tested the learning behavior of 3- and 12-month-old mice. The 12-month-old mice exhibited decreased cognitive behavior in the novel object recognition (NOR) and Y-maze tests, as indicated by decreasing interest in new objects and reducing sense of the spatial direction (Figure 1A). Our results are consistent with the prior literature.[21,26] Due to the fact that chronic inflammation may cause cognitive impairment, we next explored the expression levels of the proteins that could drive inflammation in the mouse hippocampus. Western blot analysis showed that the aged mice had a higher VCAM1 level compared with the young mice. Likewise, there were higher expressions of IBA1 (a specific microglia marker) and CD68 (an activation marker of microglia) in the aged mouse hippocampus. We also observed the total levels of TNF-α and IL-1β in the aged mouse hippocampus were significantly higher than those of the young mice (Figures 1B and 1C). In order to identify which organ(s) make major contribution to chronic peripheral inflammation in the aged mice, several organs were collected to see if there were signs of inflammation. It was observed that inflammatory factors such as NLRP3, MMP9, IL-6, IL-1β, and TNF-α were increased mainly in the aged liver, while NLRP3 and IL-1β were also increased in the kidney of the elderly mice. However, there were no obvious phenomena in the spleen, lung, or small intestine. (Figures 1D, S1A, and S1B).

To describe the differences of inflammatory manifestations during different periods of life. We analyzed the transcriptome data of human hippocampi (GSE11882), which were divided into the young (<44 years old) and elderly (>60 years old) groups. In aged human hippocampus, the significantly altered genes were associated with neurodegeneration (e.g., *SERPINA3*, *PYCARD*, *GPNMB*, *C1R*),[27–30] neuroinflammation (e.g., *CD74*, *CD86*, *TYROBP*)[31–33](Figure 1E). Then, we used the RNA-seq data from GTEx dataset to analyze the transcript expressions of liver macrophages between the young adults (aged 20–39 years) and elderly individuals (aged 60–79 years). Our results showed that the transcription of M0-and M2-type macrophages did not change with aging, but the pro-inflammatory M1 type macrophages increased significantly in the elderly group (Figure 1F). This is consistent with our animal experimental results.

β-chitosan supplementation ameliorated cognitive impairment and reduced peripheral inflammation in aged mice

We hypothesized that inflammation of the aging liver may affect neuroinflammation through the blood circulation. To test this hypothesis, we took advantage of β-chitosan (βChts) to reduce chronic peripheral inflammation (Figure 2A). 3- and 12-month-old mice (specific pathogen-free, SPF) were given different doses of βChts (Figure 2B). After a 4-week gavage administration, the mice were then evaluated for cognitive and spatial learning performance in the NOR and Y-maze tests. βChts treatment exhibited a significant ameliorative effect on reversing cognition impairment. The aged mice showed a recovery of cognitive level, which was very close to the young mice. Compared with 50 mg/kg βChts, the 100 mg/kg βChts treatment exhibited a better reversal efficiency (Figures 2C and 2D). Next, we measured the concentrations of TNF-α and IL-1β in the plasma. In line with the previous reports,[34–36] aged mice showed a significant increase in plasma levels of TNF-α and IL-1β. We observed that βChts could diminish the increment of TNF-α and IL-1β caused by aging (Figure 2E). Similarly, the age-related increases of TNF-α and IL-1β in the mouse liver were also reduced by the βChts treatment (Figures 2F and 2G). Meanwhile, we found that the expressions of TNF-α and IL-1β in other organs were not significantly affected by βChts (Figures S1C–S1F). To assess the cause of liver TNF-α and IL-1β alteration in the aging process, we did immunostaining and revealed a rise of the TNF-α, IL-1β and F4/80 (a liver macrophage marker) staining in aged mouse liver, and the expressions of these proteins were reduced by βChts supplementation. In addition, the co-positioning of most TNF-α and IL-1β with F4/80 is obvious (Figures 2H and S2A). Thus, we deemed that the number of liver macrophages increases

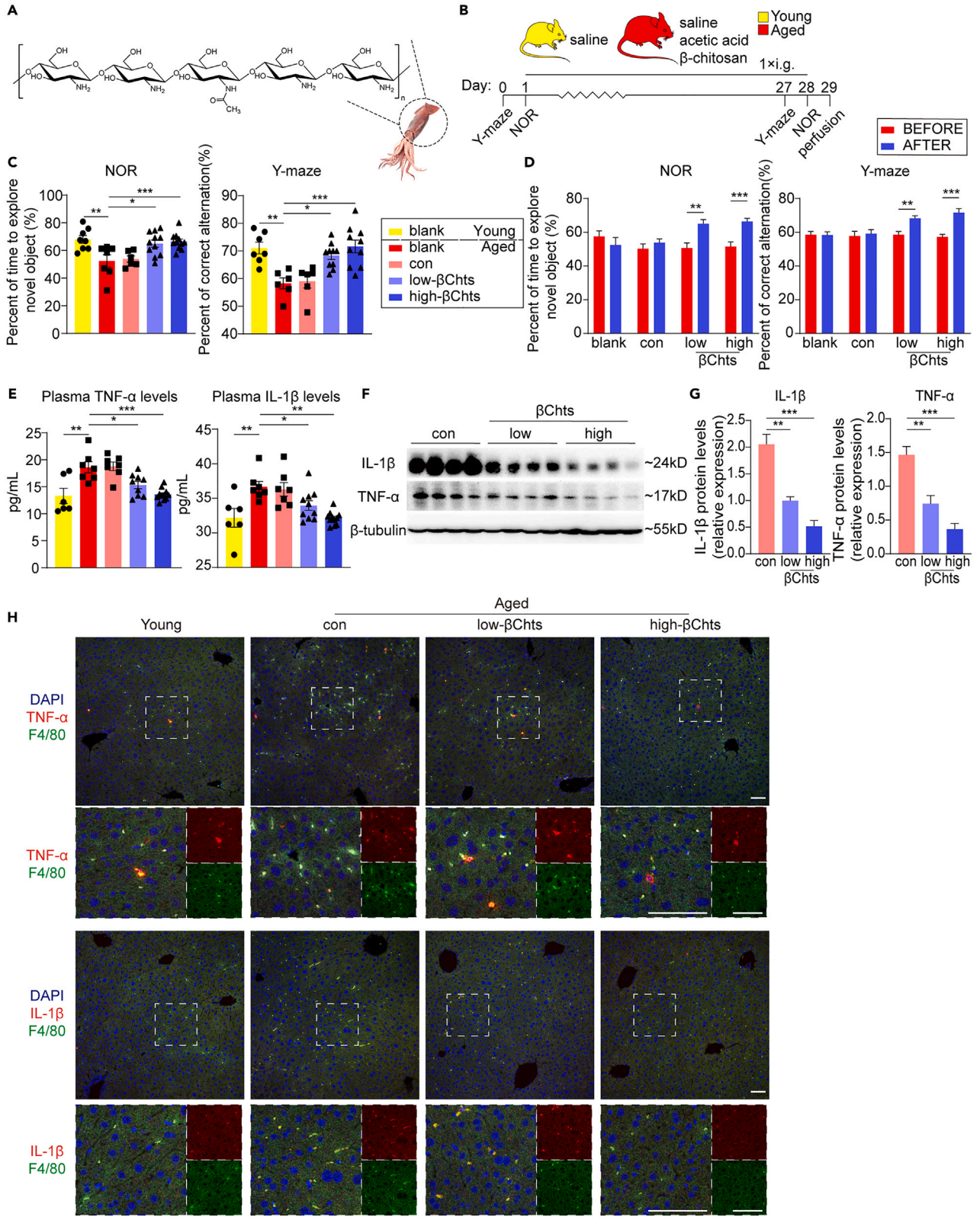
A
B
saline
saline
acetic acid
β-chitosan
1×i.g.
Young
Aged
Day: 0 1 27 28 29
Y-maze
NOR
Y-maze
NOR
perfusion
BEFORE
AFTER
C
NOR
Y-maze
Percent of time to explore novel object (%)
Percent of correct alternation(%)
blank Young
blank Aged
con
low-βChts
high-βChts
D
NOR
Y-maze
Percent of time to explore novel object (%)
Percent of correct alternation(%)
blank con low high
βChts
E
Plasma TNF-α levels
Plasma IL-1β levels
pg/mL
F
βChts
con low high
IL-1β
TNF-α
β-tubulin
~24kD
~17kD
~55kD
G
IL-1β
TNF-α
IL-1β protein levels (relative expression)
TNF-α protein levels (relative expression)
con low high
βChts
H
Young
Aged
con
low-βChts
high-βChts
DAPI
TNF-α
F4/80
TNF-α
F4/80
DAPI
IL-1β
F4/80
IL-1β
F4/80

Figure 2. β-chitosan supplementation ameliorated cognitive impairment and reduced peripheral inflammation in aged mice

(A) Chemical structure of β-chitosan (βChts, extracted from squid parietal bone).

(B) Experimental design. Young mice (yellow) were regarded as a young blank group (0.9% saline administration; 3 months old; $n = 8$). Aged mice (red) were divided into blank (0.9% saline; 12 months old; $n = 8$), control (0.35% acetic acid; 12 months old; $n = 8$), low (50 mg/kg β-chitosan contains 0.35% acetic acid; 12 months old; $n = 12$) and high (100 mg/kg β-chitosan contains 0.35% acetic acid; 12 months old; $n = 12$) concentration β-chitosan groups.

(C) The cognitive differences of novel object recognition (NOR) and Y-maze in young-blank (4 months old) and aged-blank/control/low/high (13 months old) groups of mice were detected. 12-month-old mice were treated with 50 and 100 mg/kg of β-chitosan.

(D) Comparison of cognitive changes in aged mice before (12-month-old) and after (13-month-old) administration in the novel object recognition and Y-maze.

(E) The TNF-α and IL-1β concentrations in plasma from young and aged treated mice as determined by ELISA.

(F and G) Immunoblotting analyses of IL-1β and TNF-α in the liver of different groups. Quantifications of protein expressions are shown in (G).

(H) Representative confocal images show the co-localization of F4/80 (green), TNF-α or IL-1β (red) in the liver of young and aged mice after treatment. DAPI labels cell nucleus. Scale bars, 50 μm. Data are presented as mean ± SEM, $*p < 0.05$, $**p < 0.01$, $***p < 0.001$ by one-way ANOVA.

during aging progression, which leads to the increased expressions of TNF-α and IL-1β. It is possible that the increases of TNF-α and IL-1β in aged mouse plasma are affected by the liver, and the effect of βChts on reducing liver inflammation indirectly decreases the circulating TNF-α and IL-1β concentrations.

β-chitosan supplementation alleviated neuroinflammation by suppressing the microglia activation in the hippocampus of aged mouse

Previous studies have suggested that circulating TNF-α and IL-1β promote VCAM1 expression in brain endothelial cells and cause neuroinflammation.[21] To test whether βChts affects neuroinflammation by reducing peripheral inflammation, we analyzed several inflammation-related factors in the aged mouse hippocampus. We observed that βChts-treatment resulted in decreased VCAM1 expression in the hippocampus as compared to those aged mice without βChts administration. Likewise, the levels of CD68 and IBA1 showed a gradual downward trend with an increase of βChts concentration. Interestingly, the levels of TNF-α and IL-1β in the hippocampus were also decreased by βChts treatment (Figures 3A and 3B). Microglial activation can be divided into two opposite types: pro-inflammatory M1 and anti-inflammatory M2.[37] According to our results and recent studies, we speculated that microglia M1-type activation tends to increase with age and βChts supplementation can reverse this phenomenon. We further investigated the inflammatory activation in the hippocampus of aged mice by immunostaining. In line with the previous findings,[21] we observed that the aged CA1 and dentate gyrus (DG) showed a higher expression of VCAM1 in the Lectin-positive blood vessels than the young group. IBA1 immunoreactivity and CD68 staining in IBA1+ microglia were both increased in the aged mice. Furthermore, βChts treatment significantly reduced the positive signals of IBA1 and CD68 in the aging CA1 and DG (Figures 3C–3F and S2B–S2D). Compared with the young hippocampus, the number of M1 microglia was increased in the aged DG as assessed by the increment of TNF-α+IBA1+ and IL-1β+IBA1+ microglia. After βChts treatment, the ratios of TNF-α and IL-1β in IBA1+ microglia were reduced significantly. Thus, our results indicated that the activation of M1 microglia in the aged DG was inhibited by systemic βChts administration (Figures S3A and S3B).

β-chitosan supplementation improved cognitive function in the elderly mice

To test whether βChts treatment is effective in elderly mice, we employed the 16-month-old mouse model, which is widely used in aging study (Figure S4A). It is surprised that βChts treatment also improved the cognition of elderly mice in the NOR and Y-maze tests (Figures S4B and S4C). We next investigated the plasma concentrations of TNF-α and IL-1β in elderly mice, and found that βChts down-regulated the levels of these pro-inflammatory cytokines (Figure S4D). In line with aged mice, βChts treatment reduced the expressions of TNF-α and IL-1β in the elderly liver, as well as the expressions of VCAM1, CD68, IBA1, TNF-α and IL-1β in the hippocampi of elderly mice (Figures S4E–S4H). In parallel, we observed that βChts reduced the signal of F4/80, as well as the co-localization of inflammatory factors with F4/80 in the livers of elderly mice (Figures S4I and S4J). The areas of CA1 and DG in βChts-treated elderly mice had a low level of VCAM1 in the Lectin+ blood vessels, and fewer signs of microglial inflammation as shown by fewer CD68+IBA1+ cells (Figures S5A–S5C). Likewise, the percentages of TNF-α+IBA1+ and IL-1β+IBA1+ microglia were decreased in the DG of elderly mice that received βChts treatment (Figures S5D and S5E).

β-chitosan supplementation prevented detrimental effects of LPS injection on young mice

Previous researches have shown that the level of plasmatic lipopolysaccharides (LPS) is elevated in aged human and animals.[38,39] Furthermore, LPS can also cause neuroinflammation and cognitive impairment.[40] To determine whether βChts could inhibit hepatitis and neuroinflammation caused by LPS, we built a low-grade inflammation mouse model by 10-day repeated spaced intraperitoneal injection with a low concentration of LPS (Figure 4A). Long-term administration of LPS caused cognitive impairment in young mice, which was effectively prevented by βChts administration (Figure 4B). Meanwhile, we observed that LPS administration increased the levels of TNF-α and IL-1β in the plasma, whereas they were reduced by βChts treatment (Figure 4C). The livers of young mice exposed to LPS had sharp increases of TNF-α and IL-1β levels, while administration of βChts also protected the livers of LPS-injected mice, as shown by reduction of F4/80 expression, as well as the reduced co-positionings of TNF-α, IL-1β and F4/80 (Figures 4D–4F and S6A). Similarly, there appeared to have increased neuroinflammation in their hippocampi, indicated by a significant increase in the expressions of VCAM1, CD68, IBA1, TNF-α and IL-1β. These effects of long-term LPS administration were ameliorated by βChts treatment (Figures 4G and 4H).

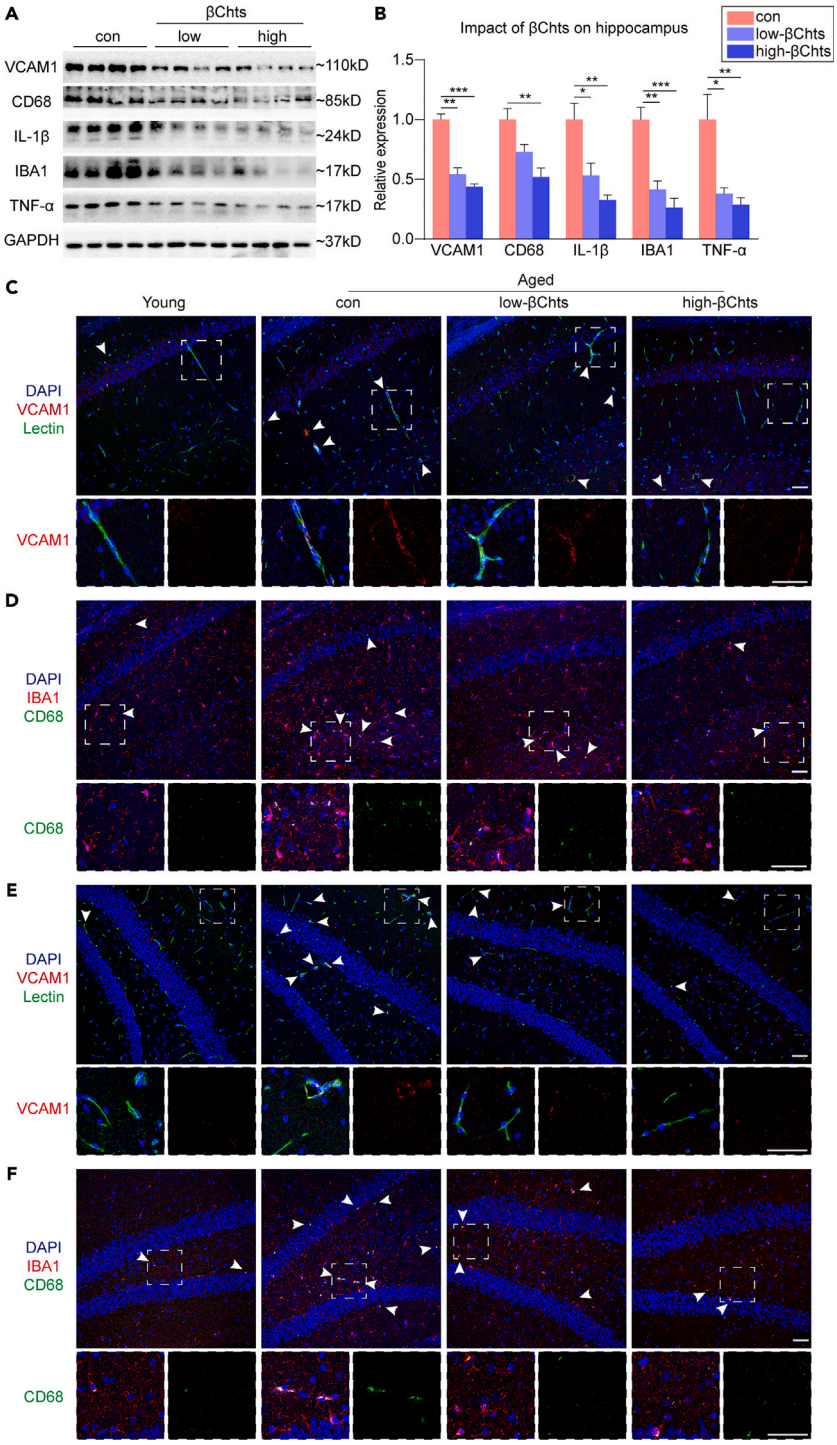

Figure 3. β-chitosan supplementation alleviated neuroinflammation by suppressing the microglia activation in the hippocampus of aged mouse

(A) Western blot analyses of VCAM1, CD68, IL-1β, IBA1 and TNF-α expressions in the hippocampi of young (4 months old) and aged (13 months old) mice after administration.

(B) Quantification analysis for the protein expressions in (A).

(C) Confocal images of VCAM1 (red) and Lectin (green) staining in the CA1 of mice treated with β-chitosan. DAPI labels cell nucleus. Arrowheads indicate VCAM1+Lectin+ vessels. Scale bars, 50 μm.

(D) Representative confocal images show the co-localization of IBA1 (red), CD68 (green) and DAPI (blue) in the CA1 of mice. Arrowheads indicate CD68+IBA1+ cells. Scale bars, 50 μm.

Figure 3. *Continued*

(E and F) VCAM1+Lectin+ vessels (E) and CD68+IBA1+ (F) microglia in the DG of mouse brain sections immunostained for VCAM1/IBA1 (red), Lectin/CD68 (green). DAPI labels cell nucleus. Arrowheads indicate the positive signal. Scale bars, 50 μm. Data are presented as mean ± SEM, $*p < 0.05$, $**p < 0.01$, $***p < 0.001$ by one-way ANOVA.

β-chitosan supplementation prevented LPS-induced neuroinflammation

The hippocampus is sensitive to the alterations caused by LPS administration. We observed a marked increase of VCAM1 expression in the Lectin+ blood vessels, and an enhanced microglial activation after LPS stimulation. In line with the aged mouse CA1 and DG, βChts treatment prevented VCAM1 up-regulation in the Lectin+ vasculature, decreased the number of microglia and their activation (Figures 5A, 5B, and S6B–S6D), significantly reduced the proportion of M1 microglia in young mice received systemic LPS administration (Figures S7A and S7B).

β-chitosan supplementation exhibited the beneficial effects on the behavioral recovery of aged/LPS-stimulated zebrafish and *Caenorhabditis elegans*

Each animal model has its unique advantages and limitations, but none can fully replicate the complexity of human physiological processes. Therefore, we chose to conduct research across multiple models to validate our findings. Zebrafish share more than 70% homologous genes with human, and they also exhibit age-related decline in cognitive function.[41,42] To test whether the overall beneficial effects of βChts treatment also occurred on zebrafish. We applied the young (with or without LPS injection) and elderly zebrafish for βChts manipulation (Figure 6A). The LPS-induced behavioral impairment of young zebrafish in the Y-maze test, was significantly more severe than the cognitive decline caused by aging. Notably, supplementation of βChts attenuated the impairment of cognitive function due to aging and LPS injection (Figure 6B). Similarly to the changes in the liver and brain of mice, βChts significantly inhibited the increase of IL-1β induced by aging and LPS injection in zebrafish (Figures 6C and 6D).

C elegans is an invertebrate model organism with a clear genetic background, encoding over 65% of homologous genes related to human diseases. *C. elegans* is widely used in several scientific research fields, such as development, aging and neurodegenerative diseases.[43,44] We next investigated how administration of βChts affects *C. elegans* in aging process and LPS stimulation (Figure 6E). Treatment with βChts increased the survival rate, body bending times and body length of aged worms. Likewise, βChts supplementation effectively prevented the LPS-induced decreases of these characteristics in young worms (Figures 6F–6I). Butanone, an innately attractive odor emitted by nutrients, is used as a stimulus in the behavior tests of *C. elegans*.[45] βChts increased the chemotaxis index (CI) in aged worms, as well as ameliorated the behavioral deficits induced by LPS in young nematodes (Figures 6J and 6K).

Impact of β-chitosan treatment on NF-κB signaling pathway in activated RAW264.7 cells

To determine whether βChts regulates the production of TNF-α and IL-1β in macrophages, we took advantage of LPS as a classic pro-inflammatory activator for macrophage, and treated LPS-stimulating RAW264.7 (a mouse leukemic monocyte/macrophage cell line) with βChts. Without LPS induction, RAW264.7 was insensitive to acetic acid or βChts (Figures S8A and S8B). Under LPS challenge, βChts treatment reduces the increments of iNOS and CD86 (both are M1-macrophage markers) in RAW264.7 cells (Figures 7A and 7B). Additionally, βChts significantly inhibited the LPS-induced increases of TNF-α and IL-1β, which were associated with up-regulation of TLR4 (Figures 7C and 7D). Consequently, the downstream molecules of NF-κB signaling pathway, p-P38, *p*-JNK and p-p65, were upregulated in the LPS-challenged group, and suppressed by βChts treatment (Figures 7E and 7F). Meanwhile, C12-sulfatide, a natural membrane glycolipid in mammals, functions as an endogenous ligand for TLR4.[46] In line with the LPS-challenged experiment, we found that βChts treatment diminished the increments of TLR4, TNF-α and IL-1β caused by C12-sulfatide stimulation in RAW264.7 cells (Figures 7G and 7H).

Docking analyses of β-chitosan and TLR4-MD-2 complex

TLR4 and MD-2 are involved in the physiological recognition of many ligands,[46–48] including LPS.[49] The binding of these activated ligands leads to the dimerization of the TLR4 extracellular domain which causes the aggregation of specific downstream proteins to its intracellular domain, resulting in a series of signal cascade reactions. Lipid A, a conserved molecular pattern, plays a central role in the immunological responses of LPS. To unveil the interaction between the TLR4-MD-2 complex and βChts, we did a ligand-protein docking calculation by using smina which is based on AutoDock Vina. Firstly, we constructed the docking conformations of LPS, 12 or 20 degree of polymerization (DP) α-chitosan (αChts)-sulfates, 12 or 21 DP βChts-sulfates , 15 DP α- or β-Chts with TLR4-MD-2 complex. We observed that the simulation results were consistent with the cell culture data of a previous report.[50] LPS and 21 DP βChts-sulfate were easier to penetrate into the pocket of MD-2 and caused the activation of TLR4-MD-2 complex (Figures 8A–8D). Secondly, we regarded the shielded pocket of MD-2 as blocked inactive conformation. βChts does not penetrate into the pocket, and prefers shielding the MD-2 pocket than other ligands (Figures 8B–8E). Moreover, the binding energy of βChts (−9∼-11 kcal/mol) is much lower than LPS (−5∼-7 kcal/mol). All these data suggested that βChts could inhibit macrophage-mediated inflammation by blocking the activation of TLR4-MD-2 complex. Because the βChts (>100 kD) we used in animal administration is much longer than the simulated 15 DP molecule, thus, there is a possibility that βChts is likely to block but not penetrate the MD-2 pocket.

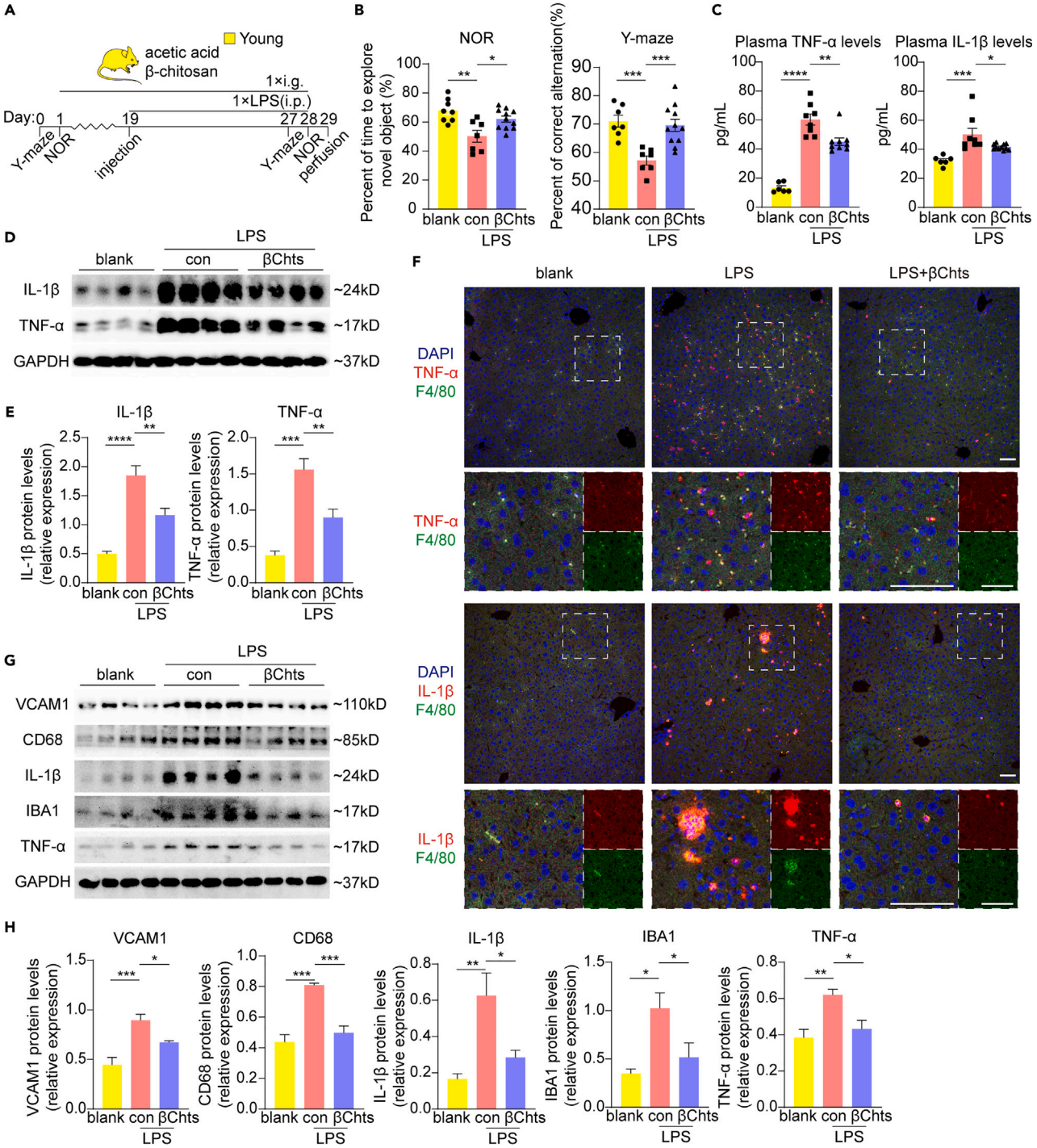

Figure 4. β-chitosan supplementation prevented detrimental effects of LPS injection on young mice

(A) Experimental design. Young mice were injected intraperitoneally with LPS (0.25 mg/kg/day) and randomly divided into control (0.35% acetic acid) and β-chitosan (100 mg/kg β-chitosan contains 0.35% acetic acid) groups.

(B) The spatial memory testing in LPS-induced mice (4 months old) by using the novel object recognition and Y-maze.

(C) IL-1β and TNF-α plasma levels from LPS-induced young mice (4 months old) after treatment.

(D and E) Immunoblotting analysis (D) and quantification (E) of IL-1β and TNF-α in the liver of LPS-challenged young mice (4 months old).

(F) Confocal co-localization analyses of F4/80 (green), TNF-α or IL-1β (red) in the liver of LPS-induced young mice (4 months old). DAPI labels cell nucleus. Scale bars, 50 μm.

Figure 4. *Continued*

(G and H) Expressions of VCAM1, CD68, IL-1β, IBA1 and TNF-α in the hippocampi of young mice (4 months old) with different treatments by western blot. Quantifications of protein expressions are shown in (H). Data are presented as mean ± SEM, *$p < 0.05$, **$p < 0.01$, ***$p < 0.001$, ****$p < 0.0001$ by one-way ANOVA.

DISCUSSION

In this study, we uncovered that aged mice exhibited chronic neuroinflammation and age-related decline in learning and memory. βChts treatment ameliorated the chronic brain inflammation and reversed the cognitive impairment, resulting in functional rejuvenation of the aged brain.

Given the well-recognized interaction effect between peripheral inflammation and central nervous system inflammation,[51–53] we proposed that age-related liver inflammation can impact brain inflammation and cognitive decline. Firstly, we found the rising levels of TNF-α and IL-1β in the aged liver were significantly correlated with the elevation of macrophages. TNF-α and IL-1β in the plasma of aged individuals were significantly increased, which might induce an up-regulation of vascular VCAM1 expression in the hippocampus, enhance M1 microglia activation, and cause brain dysfunction. These observations were in line with recent studies about the interactions between inflammatory factors in the peripheral organs, circulatory system and nervous system.[21,36,54] We found that the inflammation in the hippocampus caused by aging was mainly located in the CA1 and DG, with no obvious phenomena in the CA3 region. However, exposure to LPS can induce inflammation in the CA3 region, potentially due to its more deleterious effects than natural aging (Figure S9). During normal aging, cognitive impairment is increased not only in aged mice, but also in aged zebrafish and *C. elegans*, which were demonstrated by the weakened spatial learning and memory performance. Moreover, we observed that there was an age-related increase of IL-1β in the liver and brain of zebrafish, and the nematodes also had a weakening physical activity. Naturally, future research is needed to refine and deepen our knowledge on these animal models.

Age-related inflammation is a powerful risk factor for overall mortality in the elderly.[55] In fact, aged individuals with higher levels of inflammatory markers are more likely to be hospitalized.[56] Increasing evidences showed that microbiota dysbiosis and barrier damage in the intestinal tract will lead to cognitive decline,[57,58] and immune cells and inflammatory factors transferred from the spleen cause brain dysfunction.[59,60] Liver-specific deletion of *IGF-I* gene also leads to cognitive impairment.[20] Although previous studies have done a lot to explore the connection between peripheral organs and the brain, our understandings of the underlying mechanisms are still limited. Our study may provide a new therapeutic solution by reducing the peripheral inflammation (such as chronic liver inflammation) to weaken the neuroinflammatory response in aging individuals.

βChts is a large molecule, which cannot cross the BBB. Therefore, βChts may function in the peripheral organ(s) and indirectly regulate the brain function. Furthermore, the levels of inflammatory factors TNF-α and IL-1β were significantly higher in the liver compared to the hippocampus in both young and aged mice, suggesting that the interaction between aging liver and brain is more likely attributed to the influence of liver inflammation on neuroinflammation (Figures S10A and S10B). The circulatory TNF-α and IL-1β can bind to their receptors on the BBB in the hippocampus, leading to vascular inflammation and thereby indirectly influencing the activation of microglia. They may also directly penetrate through the highly permeable vascular regions and bind to the receptors expressing on microglia (Figure S10C). In this study, we found that βChts effectively adjusted the abnormal increase of macrophages in the aged liver, reduced the concentrations of TNF-α and IL-1β in the circulatory system. It also reduced neuroinflammation caused by vascular VCAM1 up-regulation and the associated M1 microglia activation in the hippocampus. The squid parietal bone was discarded as leftover materials from marine food processing activities. Thus, the use of underutilized species and processing discards to develop new products (e.g., βChts) is very important in the world marine food industry.

Toll-like receptors are evolutionarily ancient proteins. Previous studies have shown that zebrafish also has TLR4 similar to mouse and human,[61] while *C. elegans* TLR promotes the function of chemosensory BAG neurons for pathogen avoidance.[62] Moreover, several significantly altered genes (e.g., *CD14*, *CD44*, *LY96*)[63–65] in the aged human hippocampus were associated with TLR4 signaling (Figure 1E). LPS and endogenous ligands (e.g., sulfatides) bind to the MD-2 hydrophobic pocket and induce dimerization of two ligand-TLR4-MD-2 complexes.[46,49] In our molecular docking simulations, we found that sulfated βChts (12 and 21DP βChts -sulfates) also bound to the hydrophobic pocket of MD-2, consistent with their pro-inflammation function in the previous research.[50] Interestingly, we observed that βChts (e.g., 15 DP βChts) preferred covering the MD-2 pocket. Thus, it seems that βChts functions as an anti-inflammatory agent by preventing the corresponding ligands from forming complexes with TLR4-MD-2 receptor. Furthermore, we noticed that α-chitosan did not display the similar cognitive improvement effect in zebrafish, which seemed coincident with the results of our molecular docking stimulations (Figures 8A and 8B). Future fluorescence resonance energy transfer and endogenous ligand experiments are needed to analyze and determine how βChts influences TLR4-MD-2 complexes. Results from this study provide important evidence that the beneficial effect of βChts relies mainly on reducing abnormal inflammation in the liver. Therefore, βChts may provide us with a powerful liver-brain anti-inflammatory strategy worthy of future research.

Emerging data have shown that VCAM1 expression is upregulated not only in aged mice, but also in several inflammatory diseases,[66–68] so we tried to discover whether βChts is also effective on other inflammatory models. We selected the LPS-induced model, in which the improvement effect of βChts was similar to the aged group. βChts reduced the levels of inflammatory factors in the liver, blood and hippocampus, as well as recovered the cognitive ability of LPS-challenged animals.

In summary, our present data suggest that the abnormal activation of macrophages in the aged liver induces a circulatory pro-inflammatory environment and may promote age-related neuroinflammation. Blocking the NF-κB signaling pathway with βChts can suppress the excessive activation of hepatic macrophage and restore brain function. Additionally, the pathophysiological effects of peripheral

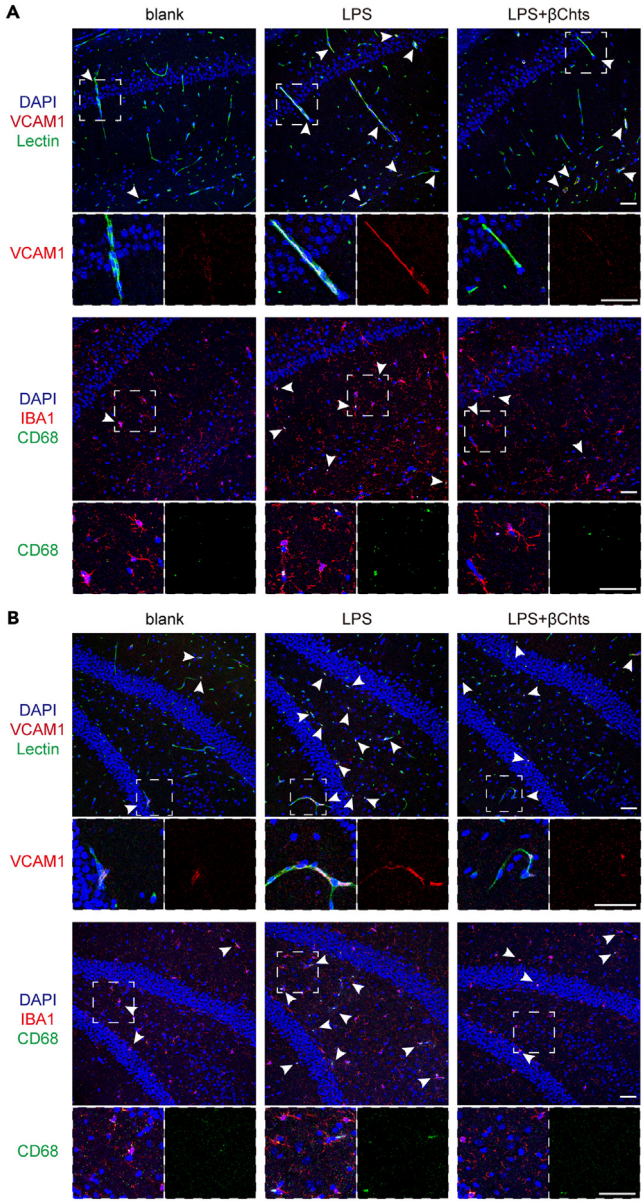

Figure 5. β-chitosan supplementation prevented LPS-induced neuroinflammation

(A) Representative confocal images show the co-localization of VCAM1+Lectin+ vessels (up) and CD68+IBA1+ cells (down) in the CA1 of LPS-challenged young mice (4 months old) after administration. DAPI labels cell nucleus. Arrowheads indicate VCAM1+Lectin+ vessels or CD68+IBA1+ cells, respectively. Scale bars, 50 μm.

(B) Immunofluorescence analysis of the co-localization of VCAM1+Lectin+ vessels and CD68+IBA1+ cells in the DG of LPS-injected young mice. DAPI labels cell nucleus. Arrowheads indicate the positive signal. Scale bars, 50 μm.

inflammation induced by LPS on brain function are also inhibited by βChts administration. Since neuroinflammation is one of the main symptoms of several brain dysfunctions, this study implies the potential of βChts in the alleviation of cognitive impairment.

Limitations of the study

Meanwhile, our study has some limitations. For example, although we had revealed the potential role of the liver in the neuroinflammation associated with aging, we have not studied all the peripheral organs. Furthermore, we found that the protein level of IL-1β was also increased in the kidney of elderly mice. In addition, neuroinflammation may in turn affect the liver, thus waiting for further exploration to understand the links connecting the liver and brain. Future research on addressing these key issues may help to better understand how the complex aging process leads to neuroinflammation and explore the broader therapeutic potential of βChts in inflammaging.

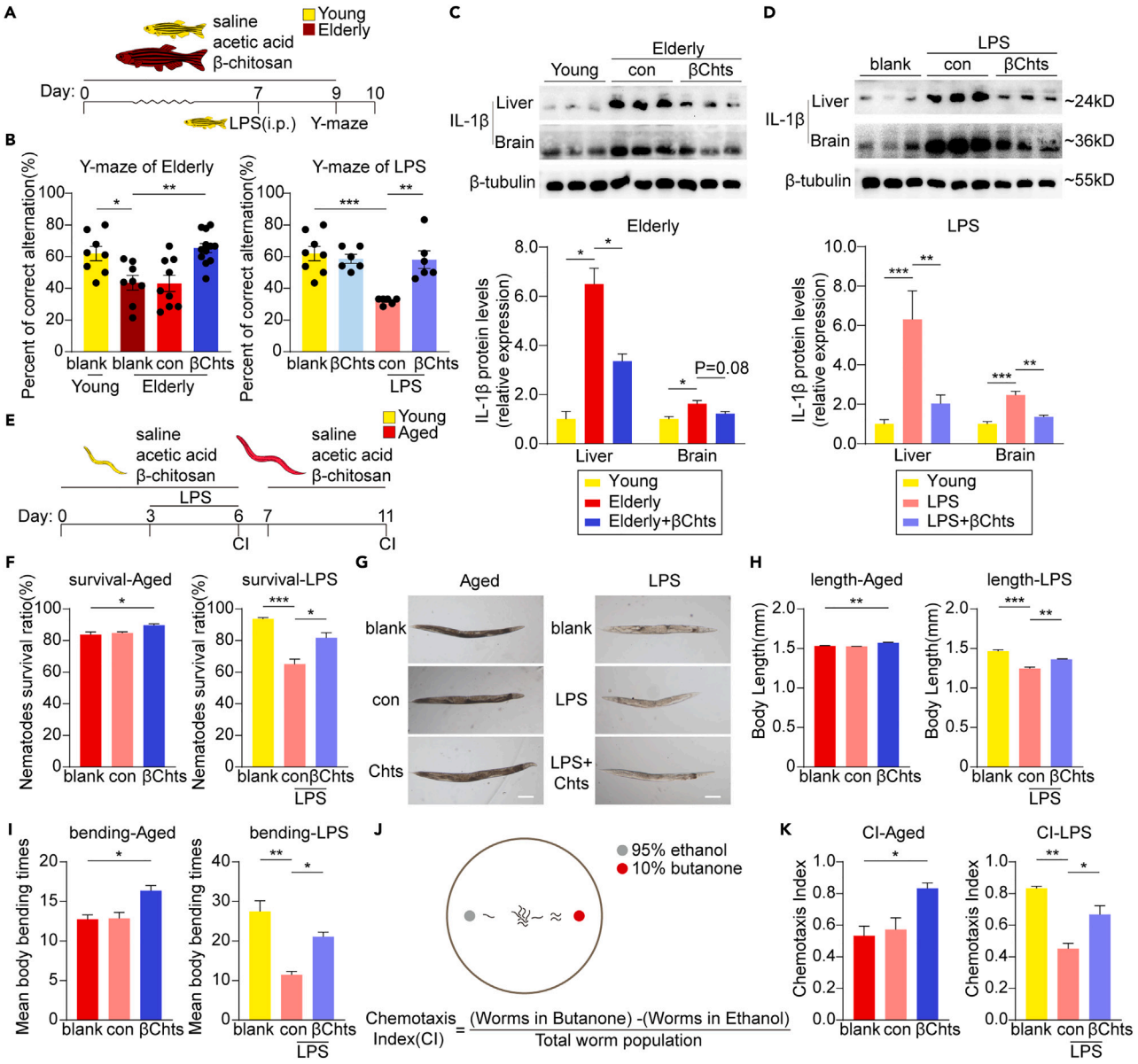

Figure 6. β-chitosan supplementation exhibited the beneficial effects on the behavioral recovery of aged/LPS-stimulated zebrafish and *C. elegans*

(A) Experimental design. Young zebrafish (4 months old; n = 8–11 per group) were randomly divided into blank, control (100 ng/mL β-chitosan contains 1.26 × 10^{-5} mL acetic acid per liter) groups and LPS-induced (1 mg/g, 10 μL) control (1.26 × 10^{-5} mL acetic acid per liter)/βChts (100 ng/mL β-chitosan contains 1.26 × 10^{-5} mL acetic acid per liter) groups. Elderly zebrafish (24 months old; n = 8–12 per group) were randomly divided into blank, control (1.26 × 10^{-5} mL acetic acid per liter), βChts (100 ng/mL β-chitosan contains 1.26 × 10^{-5} mL acetic acid per liter) groups.

(B) Correct choices in the Y-maze for young zebrafish with or without LPS administration (4 months and 10 days old) and elderly (24 months and 10 days old) zebrafish.

(C and D) Immunoblotting analysis (up) and quantification (down) of the IL-1β in different groups of young and elderly zebrafish liver and brain with β-chitosan treatment.

(E) Experimental design. Young nematodes (3 days old; n = 300/group) were divided into blank (0.9% saline), control (1.26 × 10^{-3} μL acetic acid per milliliter and 10 μg/mL LPS) and treatment (10 μg/mL β-chitosan, 1.26 × 10^{-3} μL acetic acid and 10 μg/mL LPS) groups. Aged nematodes (7 days old; n = 300/group) were divided into blank (0.9% saline), control (1.26 × 10^{-3} μL acetic acid per milliliter) and β-chitosan (10 μg/mL β-chitosan and 1.26 × 10^{-3} μL acetic acid) groups.

(F–K) Effect of β-chitosan on LPS-induced and aged nematodes. (F) Survival rate of different nematode groups (n = 195–281); (G, H) Body length of different groups (n = 40–45); (I) Body bending frequency of nematodes in different groups (n = 40–45); (J, K) Chemotaxis indices of nematodes in different groups (n = 42–140) were calculated as indicated by (J). Scale bars, 200 μm. Data are presented as mean ± SEM, *p < 0.05, **p < 0.01, ***p < 0.001 by one-way ANOVA.

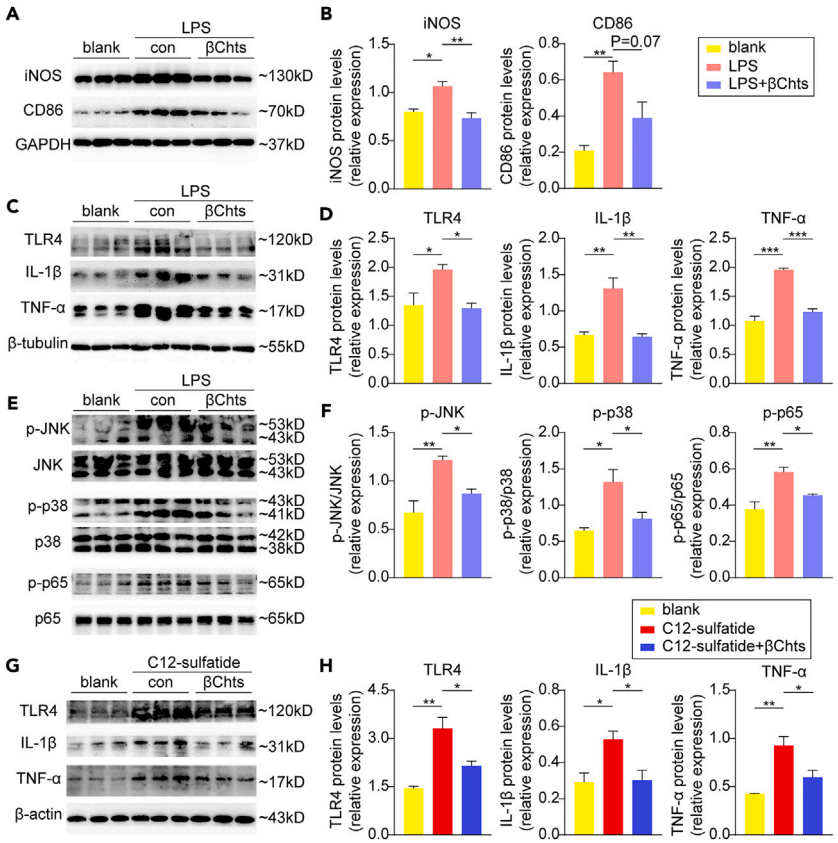

Figure 7. Immunoblotting analysis of β-chitosan treatment on NF-κB signaling pathway in activated RAW264.7 cells

(A and B) Immunoblotting analyses of the effects of β-chitosan on iNOS and CD86 in RAW264.7 cells with LPS stimulation (10 μg/mL). Quantifications of protein expressions are shown in (B).

(C and D) Effect of β-chitosan on the expressions of TLR4, TNF-α and IL-1β in RAW264.7 under LPS stimulation. (E, F) The downstream signal molecules (*p*-JNK, p-p38 and p-p65) of NF-κB in RAW264.7 (stimulated by LPS) were regulated by β-chitosan.

(G and H) Immunoblotting analysis (G) and quantification (H) of the effects of β-chitosan on TLR4, TNF-α and IL-1β in RAW264.7 cells with C12-sulfatide stimulation (10 μg/mL).

Data are presented as mean ± SEM, $*p < 0.05$, $**p < 0.01$, $***p < 0.001$ by one-way ANOVA.

RESOURCE AVAILABILITY

Lead contact

Further information and requests for resources and reagents should be directed to and will be fulfilled by the lead contact, S.Z. (qiezihoutu@126.com).

Materials availability

This study did not generate new unique reagents.

Data and code availability

- Original Western blot images have been deposited at Mendeley and are publicly available as of the date of publication. The DOI is listed in the key resources table. Microscopy data reported in this paper will be shared by the lead contact upon request.
- This paper does not report original code.
- Any additional information required to reanalyze the data reported in this paper is available from the lead contact upon request.

ACKNOWLEDGMENTS

We are grateful to the members of Mushroom Industry Center for the discussion and technical assistance. This research was funded by grants from General Program of the National Natural Science Foundation of China (No. 32370888), and from Natural Science Foundation of Fujian Province (No. 2022J05179), and from Cultivation project of Minnan Normal University (No. MSPY202101), and from Principal Project of Minnan Normal University (No. KJ2020015).

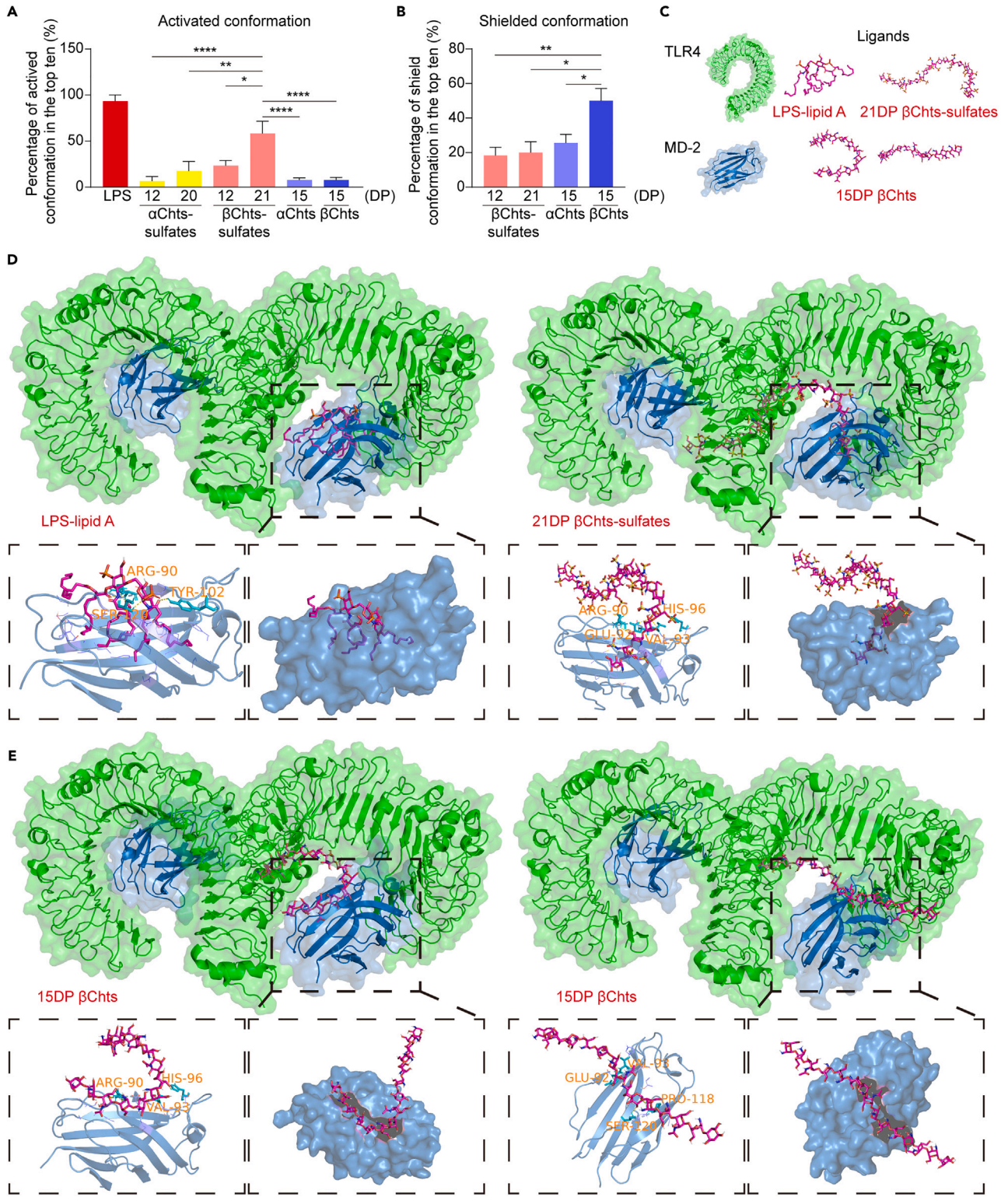

Figure 8. Docking analyses of β-chitosan and TLR4-MD-2 complex

(A and B) The proportions of activated conformation (A) and shielded conformation (B) in the top ten of molecular docking-based binding energies of different groups. αChts: α-chitosan; βChts: β-chitosan. Data are presented as mean ± SEM, *$p < 0.05$, **$p < 0.01$, ****$p < 0.0001$ by one-way ANOVA.

Figure 8. *Continued*

(C) The images show the split of each structure in TLR4-MD-2-ligands complex, TLR4 (green), MD-2 (blue) and Ligands (pink).

(D) LPS-lipid A (up) and 21DP β-chitosan-sulfate (down) penetrated and combined MD-2 pocket to form activated conformations.

(E) 15DP β-chitosan blocked and bound to the outside of the MD-2 pocket to form shield conformations.

AUTHOR CONTRIBUTIONS

C.M.Z.: Conceptualization, Data Curation, Formal Analysis, Methodology, Project Administration, Resources, Validation, Visualization, Writing – original draft. R.H.C: Project Administration, Investigation, Methodology. Y.B.L.: Project Administration, Validation, Visualization. Y.X.: Methodology, Resources. G.G.Z.: Methodology, Resources. G.A.: Methodology. Y.T.P.: Methodology, Resources, Supervision. S.G.Z.: Conceptualization, Data Curation, Formal Analysis, Funding Acquisition, Investigation, Resources, Supervision, Writing – review and editing.

DECLARATION OF INTERESTS

The authors declare that they have no competing interests.

STAR★METHODS

Detailed methods are provided in the online version of this paper and include the following:

- KEY RESOURCES TABLE
- EXPERIMENTAL MODEL AND STUDY PARTICIPANT DETAILS
- METHOD DETAILS
  - β-chitosan treatment and LPS/C12-sulfatide induction
  - Behavioral tests
  - Tissue processing
  - Measurement of plasma cytokines
  - Western blotting
  - Immunofluorescence and immunohistochemical staining
  - Cell culture and groups
  - Molecular docking
  - Bioinformatics analysis
- QUANTIFICATION AND STATISTICAL ANALYSIS

SUPPLEMENTAL INFORMATION

Supplemental information can be found online at https://doi.org/10.1016/j.isci.2024.110766.

Received: March 20, 2024
Revised: July 13, 2024
Accepted: August 15, 2024
Published: August 20, 2024

REFERENCES

1. Partridge, L., Deelen, J., and Slagboom, P.E. (2018). Facing up to the global challenges of ageing. Nature *561*, 45–56. https://doi.org/10.1038/s41586-018-0457-8.
2. Wyss-Coray, T. (2016). Ageing, neurodegeneration and brain rejuvenation. Nature *539*, 180–186. https://doi.org/10.1038/nature20411.
3. Christian, K.M., Song, H., and Ming, G.L. (2014). Functions and dysfunctions of adult hippocampal neurogenesis. Annu. Rev. Neurosci. *37*, 243–262. https://doi.org/10.1146/annurev-neuro-071013-014134.
4. Lazarov, O., and Hollands, C. (2016). Hippocampal neurogenesis: Learning to remember. Prog. Neurobiol. *138–140*, 1–18. https://doi.org/10.1016/j.pneurobio.2015.12.006.
5. Finger, C.E., Moreno-Gonzalez, I., Gutierrez, A., Moruno-Manchon, J.F., and McCullough, L.D. (2022). Age-related immune alterations and cerebrovascular inflammation. Mol. Psychiatr. *27*, 803–818. https://doi.org/10.1038/s41380-021-01361-1.
6. Trefts, E., Gannon, M., and Wasserman, D.H. (2017). The liver. Curr. Biol. *27*. R1147-r1151. https://doi.org/10.1016/j.cub.2017.09.019.
7. Cheng, M.L., Nakib, D., Perciani, C.T., and MacParland, S.A. (2021). The immune niche of the liver. Clin. Sci. *135*, 2445–2466. https://doi.org/10.1042/cs20190654.
8. Lopez, B.G., Tsai, M.S., Baratta, J.L., Longmuir, K.J., and Robertson, R.T. (2011). Characterization of Kupffer cells in livers of developing mice. Comp. Hepatol. *10*, 2. https://doi.org/10.1186/1476-5926-10-2.
9. Krenkel, O., and Tacke, F. (2017). Liver macrophages in tissue homeostasis and disease. Nat. Rev. Immunol. *17*, 306–321. https://doi.org/10.1038/nri.2017.11.
10. Peiseler, M., Araujo David, B., Zindel, J., Surewaard, B.G.J., Lee, W.Y., Heymann, F., Nusse, Y., Castanheira, F.V.S., Shim, R., Guillot, A., et al. (2023). Kupffer cell-like syncytia replenish resident macrophage function in the fibrotic liver. Science (New York, N.Y.) *381*, eabq5202. https://doi.org/10.1126/science.abq5202.
11. Cheng, K., Cai, N., Zhu, J., Yang, X., Liang, H., and Zhang, W. (2022). Tumor-associated macrophages in liver cancer: From mechanisms to therapy. Cancer Commun. *42*, 1112–1140. https://doi.org/10.1002/cac2.12345.
12. Tacke, F. (2017). Targeting hepatic macrophages to treat liver diseases. J. Hepatol. *66*, 1300–1312. https://doi.org/10.1016/j.jhep.2017.02.026.
13. Tao, L., Yi, Y., Chen, Y., Zhang, H., Orning, P., Lien, E., Jie, J., Zhang, W., Xu, Q., Li, Y., et al. (2021). RIP1 kinase activity promotes steatohepatitis through mediating cell death and inflammation in macrophages. Cell Death Differ. *28*, 1418–1433. https://doi.org/10.1038/s41418-020-00668-w.
14. Franceschi, C., Garagnani, P., Parini, P., Giuliani, C., and Santoro, A. (2018). Inflammaging: a new immune-metabolic viewpoint for age-related diseases. Nat. Rev. Endocrinol. *14*, 576–590. https://doi.org/10.1038/s41574-018-0059-4.
15. Weinstein, G., Zelber-Sagi, S., Preis, S.R., Beiser, A.S., DeCarli, C., Speliotes, E.K., Satizabal, C.L., Vasan, R.S., and Seshadri, S. (2018). Association of Nonalcoholic Fatty Liver Disease With Lower Brain Volume in Healthy Middle-aged Adults in the Framingham Study. JAMA Neurol. *75*, 97–104. https://doi.org/10.1001/jamaneurol.2017.3229.
16. Seo, S.W., Gottesman, R.F., Clark, J.M., Hernaez, R., Chang, Y., Kim, C., Ha, K.H.,

Guallar, E., and Lazo, M. (2016). Nonalcoholic fatty liver disease is associated with cognitive function in adults. Neurology *86*, 1136–1142. https://doi.org/10.1212/wnl.0000000000002498.

17. Córdoba, J., Flavià, M., Jacas, C., Sauleda, S., Esteban, J.I., Vargas, V., Esteban, R., and Guardia, J. (2003). Quality of life and cognitive function in hepatitis C at different stages of liver disease. J. Hepatol. *39*, 231–238. https://doi.org/10.1016/s0168-8278(03)00189-2.
18. Jiang, R., Wu, J., Rosenblatt, M., Dai, W., Rodriguez, R.X., Sui, J., Qi, S., Liang, Q., Xu, B., Meng, Q., et al. (2023). Elevated C-reactive protein mediates the liver-brain axis: a preliminary study. EBioMedicine *93*, 104679. https://doi.org/10.1016/j.ebiom.2023.104679.
19. Bosoi, C.R., Zwingmann, C., Marin, H., Parent-Robitaille, C., Huynh, J., Tremblay, M., and Rose, C.F. (2014). Increased brain lactate is central to the development of brain edema in rats with chronic liver disease. J. Hepatol. *60*, 554–560. https://doi.org/10.1016/j.jhep.2013.10.011.
20. Trejo, J.L., Piriz, J., Llorens-Martin, M.V., Fernandez, A.M., Bolós, M., LeRoith, D., Nuñez, A., and Torres-Aleman, I. (2007). Central actions of liver-derived insulin-like growth factor I underlying its pro-cognitive effects. Mol. Psychiatr. *12*, 1118–1128. https://doi.org/10.1038/sj.mp.4002076.
21. Yousef, H., Czupalla, C.J., Lee, D., Chen, M.B., Burke, A.N., Zera, K.A., Zandstra, J., Berber, E., Lehallier, B., Mathur, V., et al. (2019). Aged blood impairs hippocampal neural precursor activity and activates microglia via brain endothelial cell VCAM1. Nat. Med. *25*, 988–1000. https://doi.org/10.1038/s41591-019-0440-4.
22. Zhou, D.Y., Wu, Z.X., Yin, F.W., Song, S., Li, A., Zhu, B.W., and Yu, L.L.L. (2021). Chitosan and Derivatives: Bioactivities and Application in Foods. Annu. Rev. Food Sci. Technol. *12*, 407–432. https://doi.org/10.1146/annurev-food-070720-112725.
23. Krishnan, S., Chakraborty, K., and Dhara, S. (2021). Biomedical potential of β-chitosan from cuttlebone of cephalopods. Carbohydr. Polym. *273*, 118591. https://doi.org/10.1016/j.carbpol.2021.118591.
24. Zhang, H., Zhang, Y., Bao, E., and Zhao, Y. (2016). Preparation, characterization and toxicology properties of α- and β-chitosan Maillard reaction products nanoparticles. Int. J. Biol. Macromol. *89*, 287–296. https://doi.org/10.1016/j.ijbiomac.2016.04.079.
25. Alitongbieke, G., Li, X.-m., Wu, Q.-C., Lin, Z.-C., Huang, J.-F., Xue, Y., Liu, J.-N., Lin, J.-M., Pan, T., Chen, Y.-X., et al. (2020). Effect of β-chitosan on the binding interaction between SARS-CoV-2 S-RBD and ACE2. Preprint at bioRxiv. https://doi.org/10.1101/2020.07.31.229781.
26. Schroer, A.B., Ventura, P.B., Sucharov, J., Misra, R., Chui, M.K.K., Bieri, G., Horowitz, A.M., Smith, L.K., Encabo, K., Tenggara, I., et al. (2023). Platelet factors attenuate inflammation and rescue cognition in ageing. Nature *620*, 1071–1079. https://doi.org/10.1038/s41586-023-06436-3.
27. Hong, S., Beja-Glasser, V.F., Nfonoyim, B.M., Frouin, A., Li, S., Ramakrishnan, S., Merry, K.M., Shi, Q., Rosenthal, A., Barres, B.A., et al. (2016). Complement and microglia mediate early synapse loss in Alzheimer mouse models. Science (New York, N.Y.) *352*, 712–716. https://doi.org/10.1126/science.aad8373.
28. Diaz-Ortiz, M.E., Seo, Y., Posavi, M., Carceles Cordon, M., Clark, E., Jain, N., Charan, R., Gallagher, M.D., Unger, T.L., Amari, N., et al. (2022). GPNMB confers risk for Parkinson's disease through interaction with α-synuclein. Science (New York, N.Y.) *377*, eabk0637. https://doi.org/10.1126/science.abk0637.
29. Liu, W., Chen, S., Rao, X., Yang, Y., Chen, X., and Yu, L. (2023). The Inflammatory Gene PYCARD of the Entorhinal Cortex as an Early Diagnostic Target for Alzheimer's Disease. Biomedicines *11*, 194. https://doi.org/10.3390/biomedicines11010194.
30. Dai, L., Gao, F., Wang, Q., Lv, X., Cheng, Z., Wu, Y., Chai, X., Zetterberg, H., Blennow, K., Levey, A.I., et al. (2023). Molecules of senescent glial cells differentiate Alzheimer's disease from ageing. J. Neurol. Neurosurg. Psychiatry *94*, 550–559. https://doi.org/10.1136/jnnp-2022-330743.
31. Plastira, I., Bernhart, E., Joshi, L., Koyani, C.N., Strohmaier, H., Reicher, H., Malle, E., and Sattler, W. (2020). MAPK signaling determines lysophosphatidic acid (LPA)-induced inflammation in microglia. J. Neuroinflammation *17*, 127. https://doi.org/10.1186/s12974-020-01809-1.
32. Jin, C., Shao, Y., Zhang, X., Xiang, J., Zhang, R., Sun, Z., Mei, S., Zhou, J., Zhang, J., and Shi, L. (2021). A Unique Type of Highly-Activated Microglia Evoking Brain Inflammation via Mif/Cd74 Signaling Axis in Aged Mice. Aging Dis. *12*, 2125–2139. https://doi.org/10.14336/ad.2021.0520.
33. Zhou, Y., Tada, M., Cai, Z., Andhey, P.S., Swain, A., Miller, K.R., Gilfillan, S., Artyomov, M.N., Takao, M., Kakita, A., and Colonna, M. (2023). Human early-onset dementia caused by DAP12 deficiency reveals a unique signature of dysregulated microglia. Nat. Immunol. *24*, 545–557. https://doi.org/10.1038/s41590-022-01403-y.
34. Kovtonyuk, L.V., Caiado, F., Garcia-Martin, S., Manz, E.-M., Helbling, P., Takizawa, H., Boettcher, S., Al-Shahrour, F., Nombela-Arrieta, C., Slack, E., and Manz, M.G. (2022). IL-1 mediates microbiome-induced inflammaging of hematopoietic stem cells in mice. Blood *139*, 44–58. https://doi.org/10.1182/blood.2021011570 %J Blood.
35. Davizon-Castillo, P., McMahon, B., Aguila, S., Bark, D., Ashworth, K., Allawzi, A., Campbell, R.A., Montenont, E., Nemkov, T., D'Alessandro, A., et al. (2019). TNF-α-driven inflammation and mitochondrial dysfunction define the platelet hyperreactivity of aging. Blood *134*, 727–740. https://doi.org/10.1182/blood.2019000200.
36. Pioli, P.D., Casero, D., Montecino-Rodriguez, E., Morrison, S.L., and Dorshkind, K. (2019). Plasma Cells Are Obligate Effectors of Enhanced Myelopoiesis in Aging Bone Marrow. Immunity *51*, 351–366.e6. https://doi.org/10.1016/j.immuni.2019.06.006.
37. Su, W., Saravia, J., Risch, I., Rankin, S., Guy, C., Chapman, N.M., Shi, H., Sun, Y., Kc, A., Li, W., et al. (2023). CXCR6 orchestrates brain CD8(+) T cell residency and limits mouse Alzheimer's disease pathology. Nat. Immunol. *24*, 1735–1747. https://doi.org/10.1038/s41590-023-01604-z.
38. Kim, K.A., Jeong, J.J., Yoo, S.Y., and Kim, D.H. (2016). Gut microbiota lipopolysaccharide accelerates inflamm-aging in mice. BMC Microbiol. *16*, 9. https://doi.org/10.1186/s12866-016-0625-7.
39. Zhang, Y., Zhang, S., Li, B., Luo, Y., Gong, Y., Jin, X., Zhang, J., Zhou, Y., Zhuo, X., Wang, Z., et al. (2022). Gut microbiota dysbiosis promotes age-related atrial fibrillation by lipopolysaccharide and glucose-induced activation of NLRP3-inflammasome. Cardiovasc. Res. *118*, 785–797. https://doi.org/10.1093/cvr/cvab114.
40. Zhao, J., Bi, W., Xiao, S., Lan, X., Cheng, X., Zhang, J., Lu, D., Wei, W., Wang, Y., Li, H., et al. (2019). Neuroinflammation induced by lipopolysaccharide causes cognitive impairment in mice. Sci. Rep. *9*, 5790. https://doi.org/10.1038/s41598-019-42286-8.
41. Howe, K., Clark, M.D., Torroja, C.F., Torrance, J., Berthelot, C., Muffato, M., Collins, J.E., Humphray, S., McLaren, K., Matthews, L., et al. (2013). The zebrafish reference genome sequence and its relationship to the human genome. Nature *496*, 498–503. https://doi.org/10.1038/nature12111.
42. Yu, L., Tucci, V., Kishi, S., and Zhdanova, I.V. (2006). Cognitive aging in zebrafish. PLoS One *1*, e14. https://doi.org/10.1371/journal.pone.0000014.
43. Shen, P., Yue, Y., Zheng, J., and Park, Y. (2018). Caenorhabditis elegans: A Convenient In Vivo Model for Assessing the Impact of Food Bioactive Compounds on Obesity, Aging, and Alzheimer's Disease. Annu. Rev. Food Sci. Technol. *9*, 1–22. https://doi.org/10.1146/annurev-food-030117-012709.
44. Shen, P., Yue, Y., and Park, Y. (2018). A living model for obesity and aging research: Caenorhabditis elegans. Crit. Rev. Food Sci. Nutr. *58*, 741–754. https://doi.org/10.1080/10408398.2016.1220914.
45. Worthy, S.E., Rojas, G.L., Taylor, C.J., and Glater, E.E. (2018). Identification of Odor Blend Used by Caenorhabditis elegans for Pathogen Recognition. Chem. Senses *43*, 169–180. https://doi.org/10.1093/chemse/bjy001.
46. Su, L., Athamna, M., Wang, Y., Wang, J., Freudenberg, M., Yue, T., Wang, J., Moresco, E.M.Y., He, H., Zor, T., and Beutler, B. (2021). Sulfatides are endogenous ligands for the TLR4-MD-2 complex. Proc. Natl. Acad. Sci. USA *118*, e2105316118. https://doi.org/10.1073/pnas.2105316118.
47. Qiang, X., Yang, W.L., Wu, R., Zhou, M., Jacob, A., Dong, W., Kuncewitch, M., Ji, Y., Yang, H., Wang, H., et al. (2013). Cold-inducible RNA-binding protein (CIRP) triggers inflammatory responses in hemorrhagic shock and sepsis. Nat. Med. *19*, 1489–1495. https://doi.org/10.1038/nm.3368.
48. Yang, J., Qin, N., Zhang, H., Yang, R., Xiang, B., and Wei, Q. (2016). Cellular uptake of exogenous calcineurin B is dependent on TLR4/MD2/CD14 complexes, and CnB is an endogenous ligand of TLR4. Sci. Rep. *6*, 24346. https://doi.org/10.1038/srep24346.
49. Park, B.S., Song, D.H., Kim, H.M., Choi, B.S., Lee, H., and Lee, J.O. (2009). The structural basis of lipopolysaccharide recognition by the TLR4-MD-2 complex. Nature *458*, 1191–1195. https://doi.org/10.1038/nature07830.
50. Yang, Y., Xing, R., Liu, S., Qin, Y., Li, K., Yu, H., and Li, P. (2018). Immunostimulatory effects of sulfated chitosans on RAW 264.7 mouse macrophages via the activation of PI3K/Akt signaling pathway. Int. J. Biol. Macromol. *108*, 1310–1321. https://doi.org/10.1016/j.ijbiomac.2017.11.042.
51. Tan, S., Chen, W., Kong, G., Wei, L., and Xie, Y. (2023). Peripheral inflammation and neurocognitive impairment: correlations,

underlying mechanisms, and therapeutic implications. Front. Aging Neurosci. *15*, 1305790. https://doi.org/10.3389/fnagi.2023.1305790.

52. S, D., T, B., J, F., A, A., A, C.-P., L, T.-G., V, H.-R., B, G.-G., N, E., M, L., and neuroinflammation, F.V.J.J.o. (2016). Infliximab reduces peripheral inflammation, neuroinflammation, and extracellular GABA in the cerebellum and improves learning and motor coordination in rats with hepatic encephalopathy. J. Neuroinflammation *13*, 245. https://doi.org/10.1186/s12974-016-0710-8.
53. Süß, P., Hoffmann, A., Rothe, T., Ouyang, Z., Baum, W., Staszewski, O., Schett, G., Prinz, M., Krönke, G., Glass, C.K., et al. (2020). Chronic Peripheral Inflammation Causes a Region-Specific Myeloid Response in the Central Nervous System. Cell Rep. *30*, 4082–4095.e4086. https://doi.org/10.1016/j.celrep.2020.02.109.
54. Duan, J.L., Liu, J.J., Ruan, B., Ding, J., Fang, Z.Q., Xu, H., Song, P., Xu, C., Li, Z.W., Du, W., et al. (2023). Age-related liver endothelial zonation triggers steatohepatitis by inactivating pericentral endothelium-derived C-kit. Nat. Aging *3*, 258–274. https://doi.org/10.1038/s43587-022-00348-z.
55. Rea, I.M., Gibson, D.S., McGilligan, V., McNerlan, S.E., Alexander, H.D., and Ross, O.A. (2018). Age and Age-Related Diseases: Role of Inflammation Triggers and Cytokines. Front. Immunol. *9*, 586. https://doi.org/10.3389/fimmu.2018.00586.
56. Giovannini, S., Onder, G., Liperoti, R., Russo, A., Carter, C., Capoluongo, E., Pahor, M., Bernabei, R., and Landi, F. (2011). Interleukin-6, C-reactive protein, and tumor necrosis factor-alpha as predictors of mortality in frail, community-living elderly individuals. J. Am. Geriatr. Soc. *59*, 1679–1685. https://doi.org/10.1111/j.1532-5415.2011.03570.x.
57. Shi, H., Yu, Y., Lin, D., Zheng, P., Zhang, P., Hu, M., Wang, Q., Pan, W., Yang, X., Hu, T., et al. (2020). β-glucan attenuates cognitive impairment via the gut-brain axis in diet-induced obese mice. Microbiome *8*, 143. https://doi.org/10.1186/s40168-020-00920-y.
58. Wang, X., Sun, G., Feng, T., Zhang, J., Huang, X., Wang, T., Xie, Z., Chu, X., Yang, J., Wang, H., et al. (2019). Sodium oligomannate therapeutically remodels gut microbiota and suppresses gut bacterial amino acids-shaped neuroinflammation to inhibit Alzheimer's disease progression. Cell Res. *29*, 787–803. https://doi.org/10.1038/s41422-019-0216-x.
59. Unger, M.S., Li, E., Scharnagl, L., Poupardin, R., Altendorfer, B., Mrowetz, H., Hutter-Paier, B., Weiger, T.M., Heneka, M.T., Attems, J., and Aigner, L. (2020). CD8(+) T-cells infiltrate Alzheimer's disease brains and regulate neuronal- and synapse-related gene expression in APP-PS1 transgenic mice. Brain Behav. Immun. *89*, 67–86. https://doi.org/10.1016/j.bbi.2020.05.070.
60. Zhang, J., Ma, L., Chang, L., Pu, Y., Qu, Y., and Hashimoto, K. (2020). A key role of the subdiaphragmatic vagus nerve in the depression-like phenotype and abnormal composition of gut microbiota in mice after lipopolysaccharide administration. Transl. Psychiatry *10*, 186. https://doi.org/10.1038/s41398-020-00878-3.
61. Loes, A.N., Hinman, M.N., Farnsworth, D.R., Miller, A.C., Guillemin, K., and Harms, M.J. (2021). Identification and Characterization of Zebrafish Tlr4 Coreceptor Md-2. J. Immunol. *206*, 1046–1057. 1950. https://doi.org/10.4049/jimmunol.1901288.
62. Brandt, J.P., and Ringstad, N. (2015). Toll-like Receptor Signaling Promotes Development and Function of Sensory Neurons Required for a C. elegans Pathogen-Avoidance Behavior. Curr. Biol. *25*, 2228–2237. https://doi.org/10.1016/j.cub.2015.07.037.
63. Regen, T., van Rossum, D., Scheffel, J., Kastriti, M.E., Revelo, N.H., Prinz, M., Brück, W., and Hanisch, U.K. (2011). CD14 and TRIF govern distinct responsiveness and responses in mouse microglial TLR4 challenges by structural variants of LPS. Brain Behav. Immun. *25*, 957–970. https://doi.org/10.1016/j.bbi.2010.10.009.
64. Wang, Y., Li, L., Wu, Y., Zhang, S., Ju, Q., Yang, Y., Jin, Y., Shi, H., and Sun, C. (2022). CD44 deficiency represses neuroinflammation and rescues dopaminergic neurons in a mouse model of Parkinson's disease. Pharmacol. Res. *177*, 106133. https://doi.org/10.1016/j.phrs.2022.106133.
65. Fang, Z., Wu, D., Deng, J., Yang, Q., Zhang, X., Chen, J., Wang, S., Hu, S., Hou, W., Ning, S., et al. (2021). An MD2-perturbing peptide has therapeutic effects in rodent and rhesus monkey models of stroke. Sci. Transl. Med. *13*, eabb6716. https://doi.org/10.1126/scitranslmed.abb6716.
66. Perner, C., Perner, F., Gaur, N., Zimmermann, S., Witte, O.W., Heidel, F.H., Grosskreutz, J., and Prell, T. (2019). Plasma VCAM1 levels correlate with disease severity in Parkinson's disease. J. Neuroinflammation *16*, 94. https://doi.org/10.1186/s12974-019-1482-8.
67. Furuta, K., Guo, Q., Pavelko, K.D., Lee, J.H., Robertson, K.D., Nakao, Y., Melek, J., Shah, V.H., Hirsova, P., and Ibrahim, S.H. (2021). Lipid-induced endothelial vascular cell adhesion molecule 1 promotes nonalcoholic steatohepatitis pathogenesis. J. Clin. Invest. *131*, e143690. https://doi.org/10.1172/jci143690.
68. Troncoso, M.F., Ortiz-Quintero, J., Garrido-Moreno, V., Sanhueza-Olivares, F., Guerrero-Moncayo, A., Chiong, M., Castro, P.F., García, L., Gabrielli, L., Corbalán, R., et al. (2021). VCAM-1 as a predictor biomarker in cardiovascular disease. Biochim. Biophys. Acta, Mol. Basis Dis. *1867*, 166170. https://doi.org/10.1016/j.bbadis.2021.166170.
69. Leger, M., Quiedeville, A., Bouet, V., Haelewyn, B., Boulouard, M., Schumann-Bard, P., and Freret, T. (2013). Object recognition test in mice. Nat. Protoc. *8*, 2531–2537. https://doi.org/10.1038/nprot.2013.155.
70. Kraeuter, A.K., Guest, P.C., and Sarnyai, Z. (2019). The Y-Maze for Assessment of Spatial Working and Reference Memory in Mice. Methods Mol. Biol. *1916*, 105–111. https://doi.org/10.1007/978-1-4939-8994-2_10.
71. Benvenutti, R., Marcon, M., Gallas-Lopes, M., de Mello, A.J., Herrmann, A.P., and Piato, A. (2021). Swimming in the maze: An overview of maze apparatuses and protocols to assess zebrafish behavior. Neurosci. Biobehav. Rev. *127*, 761–778. https://doi.org/10.1016/j.neubiorev.2021.05.027.
72. Chandra, R., Farah, F., Muñoz-Lobato, F., Bokka, A., Benedetti, K.L., Brueggemann, C., Saifuddin, M.F.A., Miller, J.M., Li, J., Chang, E., et al. (2023). Sleep is required to consolidate odor memory and remodel olfactory synapses. Cell *186*, 2911–2928.e2920. https://doi.org/10.1016/j.cell.2023.05.006.
73. Chu, Q., Jia, R., Chen, M., Li, Y., Yu, X., Wang, Y., Chen, W., Ye, X., Liu, Y., Jiang, Y., and Zheng, X. (2019). Tetrastigma hemsleyanum tubers polysaccharide ameliorates LPS-induced inflammation in macrophages and Caenorhabditis elegans. Int. J. Biol. Macromol. *141*, 611–621. https://doi.org/10.1016/j.ijbiomac.2019.09.039.
74. Li, X., Wang, X., Wang, K., Yang, X., Liu, X., Chen, J., Li, J., Wang, J., Guo, Q., and Wang, H. (2023). Black rice anthocyanin extract enhances the antioxidant capacity in PC12 cells and improves the lifespan by activating IIS pathway in Caenorhabditis elegans. Comp. Biochem. Physiol. C Toxicol. Pharmacol. *265*, 109533. https://doi.org/10.1016/j.cbpc.2022.109533.
75. Sturm, G., Finotello, F., and List, M. (2020). Immunedeconv: An R Package for Unified Access to Computational Methods for Estimating Immune Cell Fractions from Bulk RNA-Sequencing Data. Methods Mol. Biol. *2120*, 223–232. https://doi.org/10.1007/978-1-0716-0327-7_16.
76. Schaum, N., Lehallier, B., Hahn, O., Pálovics, R., Hosseinzadeh, S., Lee, S.E., Sit, R., Lee, D.P., Losada, P.M., Zardeneta, M.E., et al. (2020). Ageing hallmarks exhibit organ-specific temporal signatures. Nature *583*, 596–602. https://doi.org/10.1038/s41586-020-2499-y.

STAR★METHODS

KEY RESOURCES TABLE

REAGENT or RESOURCE	SOURCE	IDENTIFIER
Antibodies		
Rabbit monoclonal anti-VCAM1	Abcam	Cat#ab134047; RRID: AB_2721053
Rabbit polyclonal anti-CD68	ProteinTech	Cat#28058-1-AP; RRID: AB_2881049
Rabbit polyclonal anti-IBA1	ProteinTech	Cat#10904-1-AP; RRID: AB_2224377
Mouse monoclonal anti-IL-1β	Santa Cruz Biotechnology	Cat#SC-52012
Rabbit polyclonal anti-TNF-α	Affinity	Cat#AF7014
Rabbit polyclonal anti-NLRP3	Affinity	Cat#DF7438; RRID: AB_2839376
Rabbit polyclonal anti-MMP9	Abmart	Cat#TA0220
Rabbit polyclonal anti-IL-6	Abmart	Cat#TD6087
Rabbit polyclonal anti-iNOS	Affinity	Cat#AF0199; RRID: AB_2833391
Rabbit polyclonal anti-CD86	Affinity	Cat#DF6332; RRID: AB_2838296
Rabbit polyclonal anti-TLR4	ProteinTech	Cat#19811-1-AP; RRID: AB_10638446
Rabbit polyclonal anti-JNK	ProteinTech	Cat#24164-1-AP; RRID: AB_2879443
Rabbit polyclonal anti-p38	ProteinTech	Cat#14064-1-AP; RRID: AB_2878007
Rabbit polyclonal anti-p65	ProteinTech	Cat#10745-1-AP; RRID: AB_2178878
Rabbit polyclonal anti-*p*-JNK	Affinity	Cat#AF3318
Rabbit polyclonal anti-p-p38	Affinity	Cat#AF4001
Rabbit polyclonal anti-p-p65	Affinity	Cat#AF2006
Rabbit polyclonal anti-IL-1β	Affinity	Cat#AF5103
Rabbit polyclonal anti-IL-1β	ProteinTech	Cat#16806-1-AP
Rabbit polyclonal anti-β-tubulin	Affinity	Cat#AF7018
Rabbit polyclonal anti-GAPDH	Affinity	Cat#AF7021; RRID: AB_2839421
Rabbit polyclonal anti-β-actin	Affinity	Cat#AF7011
Mouse monoclonal anti-F4/80	Santa Cruz Biotechnology	Cat#SC-377009; RRID: AB_2927461
Mouse monoclonal anti-CD68	Novus Biologicals	Cat#NB100-683
Mouse monoclonal anti-TNF-α	ProteinTech	Cat#60291-1-Ig
Lycopersicon Esculentum (Tomato) Lectin (LEL, TL), DyLight® 488 (DL-1174-1)	Vector Laboratories	Cat#DL-1174; RRID: AB_2336404
Alexa Fluor® 594-conjugated AffiniPure™ Donkey Anti-Rabbit IgG (H + L)	Jackson	Cat#711-585-152; RRID: AB_2340621
Alexa Fluor® 488-conjugated AffiniPure™ Donkey Anti-Mouse IgG (H + L)	Jackson	Cat#715-545-150; RRID: AB_2340846
Goat anti-Rabbit IgG F(ab')2 Secondary Antibody	ThermoFisher Scientific	Cat#31234; RRID: AB_228343
Goat anti-Mouse IgG F(ab')2 Secondary Antibody	ThermoFisher Scientific	Cat#31166; RRID: AB_228309
Chemicals, peptides, and recombinant proteins		
Lipopolysaccharides (LPS)	sigma	Cat#L2880
tricaine MS-222	sigma	Cat#A-5040
C12-sulfatide	Avanti	Cat#131305

(*Continued on next page*)

Continued

REAGENT or RESOURCE	SOURCE	IDENTIFIER
Tetramisole hydrochloride	aladdin	Cat#T335508
Avertin	sigma	Cat#T48402
RIPA lysis buffer	Beyotime Biotechnology	Cat#P0013
Protease inhibitors	Roche	Cat#04693132001
Phosphatase inhibitors	Roche	Cat#04906 837001
PVDF membrane	Roche	Cat#03010040001
EDTA antigen retrieval (pH = 9.0)	ZSGB-BIO	Cat#ZLI-9069
Donkey serum	MeilunBio	Cat#MB4516-1
DAPI Staining Solution	Beyotime Biotechnology	Cat#C1005
Fluoromount-G® Anti-Fade	Southernbiotech	Cat#0100-35
Goat serum	MeilunBio	Cat#MB4508-1
β-Chitosan	Mengdeer Biotechnology (Xiamen, China)	N/A
DMEM	Gibco	Cat#C11995500BT
FBS	Cegrogen	Cat#A0500-3011
Penicillin-streptomycin	Cytiva	Cat#SV30010
Critical commercial assays		
Mouse TNF-α High Sensitivity ELISA	Multi Sciences	Cat#70-EK282HS/3-96
Mouse IL-1β High Sensitivity ELISA	Multi Sciences	Cat#70-EK201BHS-96
Pierce™ BCA Protein Assay Kits	ThermoFisher Scientific	Cat#23227
Enhanced HRP Chromogenic Substrate Kit (Rabbit)	ZSGB-BIO	Cat#PV-9001
Enhanced HRP Chromogenic Substrate Kit (Mouse)	ZSGB-BIO	Cat#PV-9002
3,30-diaminobenzidine (DAB) staining kit	ZSGB-BIO	Cat#ZLI-9019
Deposited data		
Western blot data	This paper	https://data.mendeley.com/datasets/w66hydtgwg/1
Experimental models: Cell lines		
RAW264.7 cells	Zhong Qiao Xin Zhou Biotechnology (Shanghai, China)	Cat#ZQ0098
Experimental models: Organisms/strains		
mouse: C57BL/6JNifdc	Charles River Laboratories	N/A
zebrafish: AB	Shanghai FishBio (Shanghai, China)	N/A
Caenorhabditis elegans: N2	C. elegans Genetics Center (University of Minnesota, MN, USA)	N/A
Software and algorithms		
RCSB database	University of California San Diego	RRID:SCR_012820; www.rcsb.org
Chemdraw 2019	CambridgeSoft	RRID:SCR_016768; http://www.perkinelmer.co.uk/category/chemdraw
PyMoL-2.5.5	DeLano Scientific LLC	RRID:SCR_000305; http://www.pymol.org/
Genotype-Tissue Expression	Broad Institute	RRID:SCR_013042; https://commonfund.nih.gov/GTEx/
Gene Expression Omnibus	National Center for Biotechnology Information	RRID:SCR_005012; https://www.ncbi.nlm.nih.gov/geo/
ImageJ 1.53e	NIH	RRID: SCR_003070; https://imagej.nih.gov/ij/
GraphPad Prism v8.0	GraphPad Software Inc	RRID: SCR_002798; http://www.graphpad.com/

EXPERIMENTAL MODEL AND STUDY PARTICIPANT DETAILS

All C57BL/6JNifdc male mice were purchased from Charles River Laboratories. The mice were maintained in environmentally controlled conditions at 22°C under a 12/12 h light/dark cycle with free access to food and water. Prior to testing, the mice were kept for at least 2 weeks and then randomly assigned to different experimental groups before treatment. Experiments include young mice (3–4 months of age), aged mice (12–13 months of age) and old mice (16–17 months of age).

Young (4 months old, both sexes) and old (24 months old, both sexes) AB zebrafish were bought from Shanghai FishBio Co., Ltd (Shanghai, China). All fish were raised at a temperature of 28.5°C under a 10/14 h light/dark cycle.

The wild-type *Caenorhabditis elegans* (N2) were maintained on nematode growth medium (NGM medium：1.5 g NaCl, 10g Agar, 1.25 g Peptone, 0.5 mL 1 M $MgSO_4$, 12.5 mL 1 M KH_2PO_4, 0.5 mL 5 mg/mL Cholesterol in 95% ETOH, 0.5 mL 1% Nystatin, 0.5 mL 1M $CaCl_2$, 1 mL 50 mg/mL Streptomycin in 1 L distilled water) with Escherichia coli OP50 at 20°C.

All the procedures related to animals in this study have been reviewed and approved by the Animal Ethics and Welfare Committee of Minnan Normal University (MNU-AEWC-2021004).

METHOD DETAILS

β-chitosan treatment and LPS/C12-sulfatide induction

β-Chitosan (>100 kD; 80% degree of deacetylation) was provided by Mengdeer Biotechnology Co., Ltd. (Xiamen, China). Mice were received low or high (50 or 100 mg/kg) β-Chitosan treatment for 28 days. Zebrafish were received 100 ng/mL β-Chitosan treatment for 10 days. *Caenorhabditis elegans* were received 10 μg/mL β-Chitosan treatment for 4 or 6 days. Then, on the 19th day after β-Chitosan administration, LPS-induced mice were injected intraperitoneally (i.p.) in a dose of 0.25 mg/kg once a day with LPS (sigma, L2880) for 10 days. On the 7th day after β-Chitosan administration, LPS-induced zebrafish were anesthetized by tricaine MS-222 (100 mg/L; sigma, A-5040) and injected intraperitoneally with 1 μg/g LPS only once. On the 3rd day after β-Chitosan administration, LPS-induced *Caenorhabditis elegans* were received LPS at 10 mg/mL for 3 days. RAW264.7 cells were received β-Chitosan (100 ng/mL), LPS (10 mg/mL) or C12-sulfatide (10 μg/mL, Avanti, 131305) for 24 h.

Behavioral tests

Novel object recognition test[69] was performed in a 40 × 40 × 40 cm open field. On day 1 of testing, put two identical Lego towers in the open field. Mice were allowed to freely explore the open field for 10 min or the Lego Towers for 20 s until either of them was satisfied. On day 2 of testing, replaced the one of two familiar objects by a novel object at the same location. Mice were allowed to explore the open field for 10 min. The new object discrimination index was calculated by using the following formula: (time interaction with novel object)/(time interaction with both objects)×100.

Y-maze test was consisted of three identical arms. Placed the animal in the start arm (A) and recorded the sequence of explored arms (such as ACBCBA). The accuracy of the Y maze was calculated by using the following formula: correct alternation (such as ABC)/the total alternation×100. Mice were allowed to freely explore the Y-maze for 8 min. The size of each arm was 30 × 15 × 7 cm.[70] Zebrafish were freed to explore the Y-maze for 5 min. The size of each arm was 25 × 15 × 8 cm.[71]

In chemotaxis assay,[72] dropped 2 mL 95% ethanol and 10% butanone (dissolved in 95% ethanol) on the NGM without food, then put the worms in the middle of the NGM and waited 1 h to record the number of worms in the two kinds of liquid respectively. The Chemotaxis Index (CI) was calculated: (worms in butanone) −(worms in ethanol)/Total worm population. Then, wash the worms with M9 buffer for three times, anesthetize the worms with tetramisole hydrochloride (aladdin, T335508), and prepare it with 1% agarose slide.[73,74]

Tissue processing

Briefly, mice were anesthetized by Avertin (2.5%, 0.018 mL/g; sigma, T48402) to collect blood (blood: sodium citrate = 1:9) and followed by PBS perfusion. Brain, liver, lung, spleen, small intestine and kidney were collected in 4% PFA or saved at - 80°C.

Measurement of plasma cytokines

According to the instructions in the Elisa manual, obtained the mice plasma samples which were used to measure TNF-α (Multi Sciences, 70-EK282HS/3–96) and IL-1β (Multi Sciences, 70-EK201BHS-96).

Western blotting

Tissues and cells were lysed and homogenized with RIPA lysis buffer (Beyotime, P0013) containing protease inhibitors (Roche, 04693132001) and phosphatase inhibitors (Roche, 04906 837001). Total protein concentration was determined by BCA assay (ThermoFisher Scientific, 23227).

Used 10%–12% SDS-PAGE to process the equal amount of protein and transferred it to PVDF membrane (Roche, 03010040001). The membranes were blocked with 5% no-fat milk/TBST at room temperature for 1 h and then incubated with the primary antibody (1:1000 dissolved in TBST, see key resources table) at 4°C for at least 17 h. The secondary antibodies (1:5000, ThermoFisher Scientific, 31234, Rabbit; 31166, Mouse) of the corresponding species were incubated at room temperature for 1 h after the first antibody was recovered, visualized by using ECL Western Boltting Substrate.

The primary antibodies for western blot, mice: VCAM1 (Abcam, ab134047, RRID:AB_2721053), CD68 (ProteinTech, 28058-1-AP), IL-1β (Santa Cruz Biotechnology, SC-52012), TNF-α (Affinity, AF7014), IBA1 (ProteinTech, 10904-1-AP), NLRP3 (Affinity, DF7438), MMP9 (Abmart, TA0220), IL-6 (Abmart, TD6087); cell: iNOS (Affinity, AF0199), CD86(Affinity, DF6332), TLR4 (ProteinTech, 19811-1-AP); JNK (ProteinTech, 24164-1-AP); p38 (ProteinTech, 14064-1-AP); p65 (ProteinTech, 10745-1-AP); *p*-JNK (Affinity, AF3318); p-p38 (Affinity, AF4001); p-p65 (Affinity, AF2006), TNF-α (Affinity, AF7014), IL-1β (Affinity, AF5103); zebrafish: IL-1β (ProteinTech, 16806-1-AP). β-tubulin (Affinity, AF7018), GAPDH (Affinity, AF7021), β-actin (Affinity, AF7011).

Immunofluorescence and immunohistochemical staining

The tissue was prepared into paraffin sections of 5 μm. The hippocampus was performed in the coronal section, and the largest lobe of the liver was performed in the horizontal section.

For immunofluorescence, after the sections were dewaxed and rehydrated, washed three times for 4 min in distilled water and then used the pH = 9.0 EDTA (ZSGB-BIO, ZLI-9069) for antigen retrieval. Sections blocked in 10% donkey serum (dissolved in TBS; MeilunBio, MB4516-1) at room temperature for 2 h and incubated with primary antibodies (1:200, also see key resources table) at 4°C for 48 h. Sections were washed five times for 4 min in TBST, incubated with the mixture of secondary antibodies (1:200; Jackson, 711-585-152, Rabbit; 715-545-150, Mouse) and DAPI (1 : 3000) at room temperature for 2 h in dark. The stained slides were mounted with anti-fade fluoromount-G (Southernbiotech, 0100-35). Images were taken on a Las X Confocal laser scanning microscopy SP8.

For immunohistochemistry, after performing antigen retrieval, the slides were treated with H_2O_2 for 15 min to inhibit endogenous peroxidase activity. Subsequently, the slides were blocked at room temperature in 10% goat serum (dissolved in TBS; MeilunBio, MB4508-1) for 2 h and incubated with the primary antibody (1:200, also see key resources table) at 4°C for 48 h. According to the instructions, incubated the slices with the secondary antibody (ZSGB-BIO, PV-9001, Rabbit; PV-9002, Mouse) and executed the visualization process utilizing the 3,30-diaminobenzidine (DAB) staining kit (ZSGB-BIO, ZLI-9019). Images were captured by a BX51 microscope (Olympus).

The primary antibodies for immunofluorescent staining, liver: F4/80 (Santa Cruz Biotechnology, SC-377009), IL-1β (Affinity, AF5103), TNF-α (Affinity, AF7014); hippocampus: VCAM1 (Abcam, ab134047), Lectin (Vector, DL-1174), IBA1 (ProteinTech, 10904-1-AP), CD68 (Novus Biologicals, NB100-683), IL-1β (Santa Cruz Biotechnology, SC-52012), TNF-α (ProteinTech, 60291-1-Ig).

The primary antibodies for immunohistochemical staining: IBA1 (ProteinTech, 10904-1-AP), CD68 (Novus Biologicals, NB100-683).

Cell culture and groups

RAW264.7 cells (mouse leukemia cells of monocyte macrophage) was purchased from Zhong Qiao Xin Zhou Biotechnology Co., Ltd (Shanghai, China). The cells were cultured in DMEM (Gibco, C11995500BT) supplemented with 10% FBS (Cegrogen, A0500-3011), and penicillin-streptomycin (100 U/ml; Cytiva, SV30010) at 37°C and 5% CO_2. The cell experiment was divided into blank, control (1.26×10^{-5} μL acetic acid per milliliter) and β-Chitosan (100 ng/mL β-chitosan contains 1.26×10^{-5} μL acetic acid per milliliter) groups with or without LPS/C12-sulfatides stimulation.

Molecular docking

The structures of LPS (PDB ID: 3FXI) and TLR4-MD-2 complex (PDB ID: 5IJB) were downloaded from RCSB database (www.rcsb.org). The structures of α/β-Chitosan and α/β-Chitosan-sulfates were constructed into a three-dimensional structure by using Chemdraw and Chem3D. Before docking, all ligands and proteins were converted by AutoDockTools 1.5.7 to PDBQT format. Molecular docking was performed using smina (based on AutoDock Vina; https://sourceforge.net/projects/smina/). The ten conformations with the lowest binding energy were selected and analyzed by PyMoL.

Bioinformatics analysis

Genotype-Tissue Expression (GTEx, https://commonfund.nih.gov/GTEx/) provides publicly available gene expression data from normal liver tissue of human. The GSE11882 (GPL570 platform) dataset was selected from the Gene Expression Omnibus (GEO) database (https://www.ncbi.nlm.nih.gov/geo/). Statistical analyses were performed using R Studio software v2023.09.0 + 463 (Posit Software, USA) and Graphpad Prism (Graphpad Software Inc, USA). Then, in the present study, the cut-off values were set at $p < 0.05$ and | log (fold change)| >1 to filter DEGs (differentially expressed genes).

Using these data, we analyzed the age-specific differences in macrophage expression in human liver tissue and the age-specific differences in gene expression in the human brain hippocampus. We utilized GENCODE v26 for annotating the RNA-Seq datasets in the GTEx database and employed the R package Immunedeconv[75] to process the CIBERSORT data (https://cibersort.stanford.edu/). Subsequently, we performed immune analysis using gene expression signatures from the official website for 22 immune cell subtypes, resulting in identification of M0, M1 and M2 types of macrophages.

Tabula Muris (https://tabula-muris.ds.czbiohub.org/) provides publicly available data on the gene expressions of TNF-α and IL-1β receptors in mouse brain endothelial cells and microglia. The data of TNF-α and IL-1β expression in the mouse liver and brain with different ages were selected from the Tabula Muris Senis (https://twc-stanford.shinyapps.io/maca/).[76]

QUANTIFICATION AND STATISTICAL ANALYSIS

In the behavioral tests, before treatment, the animals were randomly divided into different groups. The slides were uniformly processed for staining and mounted with anti-fade fluoromount-G. During the imaging process, the slides of different groups were imaged under the same confocal parameters, and the entire imaging procedure was completed within a short time frame. The results of immunofluorescent staining and western blot were analyzed by ImageJ. The western blot images calculated the grayscale value, while the immunofluorescent staining images calculated the area of the fluorescence intensity. Data were analyzed with GraphPad Prism v8.0 software for two-tailed t test for two group comparisons, and one-way ANOVA for three or more comparisons. All the data with error bar are represented by meas ± SEM. $p < 0.05$ was considered to be statistically significant.